Pseudo-Calibration: Improving Predictive Uncertainty Estimation in Unsupervised Domain Adaptation

Dapeng Hu [1] **Jian Liang** [2 3] **Xinchao Wang** [4] **Chuan-Sheng Foo** [5 1]

Abstract

Unsupervised domain adaptation (UDA) has seen substantial efforts to improve model accuracy for an unlabeled target domain with the help of a labeled source domain. However, UDA models often exhibit poorly calibrated predictive uncertainty on target data, a problem that remains under-explored and poses risks in safety-critical UDA applications. The calibration problem in UDA is particularly challenging due to the absence of labeled target data and severe distribution shifts between domains. In this paper, we approach UDA calibration as a target-domain-specific unsupervised problem, different from mainstream solutions based on *covariate shift*. We introduce Pseudo-Calibration (PseudoCal), a novel post-hoc calibration framework. Our innovative use of inference-stage *mixup* synthesizes a labeled pseudo-target set capturing the structure of the real unlabeled target data. This turns the unsupervised calibration problem into a supervised one, easily solvable with *temperature scaling*. Extensive empirical evaluations across 5 diverse UDA scenarios involving 10 UDA methods consistently demonstrate the superior performance and versatility of PseudoCal over existing solutions. Code is available at `https://github.com/LHXXHB/PseudoCal`.

1. Introduction

Unsupervised domain adaptation (UDA) (Pan & Yang, 2009) has been widely studied for enhancing the generalization of deep learning models (He et al., 2016) from labeled source domains to an unlabeled target domain with similar tasks but varying data distributions. Notable progress has been achieved in developing effective UDA methods (Ganin & Lempitsky, 2015), practical applications (Tsai et al., 2018), and real-world settings (Liang et al., 2020a), with a predominant focus on target domain model accuracy.

However, for a classification model, achieving reliable predictive uncertainty estimation is as crucial as high accuracy, especially in safety-critical decision-making scenarios like autonomous driving and medical diagnosis (Guo et al., 2017). A calibrated model should produce probability predictions that accurately reflect correctness likelihood (Guo et al., 2017). Although predictive uncertainty calibration has garnered substantial attention in IID supervised learning tasks with deep models (Thulasidasan et al., 2019), the calibration problem in UDA remained largely unexplored until a pioneering UDA study (Wang et al., 2020), which revealed that improved UDA model accuracy comes at the expense of poor uncertainty calibration on target data. This phenomenon is vividly illustrated in Figure 1(a), where increasing target domain accuracy is accompanied by significant overfitting of the negative log-likelihood (NLL) loss during adaptation. The first challenge with UDA calibration is the absence of labeled data in the target domain, rendering the direct leverage of supervised IID calibration methods like *temperature scaling* (Guo et al., 2017) impossible. Another significant challenge arises from severe domain distribution shifts between source and target. Consequently, UDA models calibrated with only labeled source data cannot ensure effective calibration for unlabeled data in the target domain (Wang et al., 2020).

To address these challenges, mainstream approaches (Park et al., 2020; Wang et al., 2020) treat calibration in UDA as a *covariate shift* problem (Sugiyama et al., 2007) across domains. They typically employ *importance weighting* (Cortes et al., 2008) to estimate weights for source samples based on the similarity to target data and then perform sample-weighted *temperature scaling* with a labeled source validation set. These solutions have obvious drawbacks that impede effective and efficient model calibration in UDA. Firstly, *importance weighting* may not be reliable under

[1]Centre for Frontier AI Research, A*STAR, Singapore [2]NLPR & MAIS, Institute of Automation, Chinese Academy of Sciences, China [3]School of Artificial Intelligence, University of Chinese Academy of Sciences [4]National University of Singapore [5]Institute for Infocomm Research, A*STAR, Singapore. Correspondence to: Dapeng Hu <lhxxhb15@gmail.com>, Chuan-Sheng Foo <chuan_sheng@i2r.a-star.edu.sg>.

Proceedings of the 41st International Conference on Machine Learning, Vienna, Austria. PMLR 235, 2024.

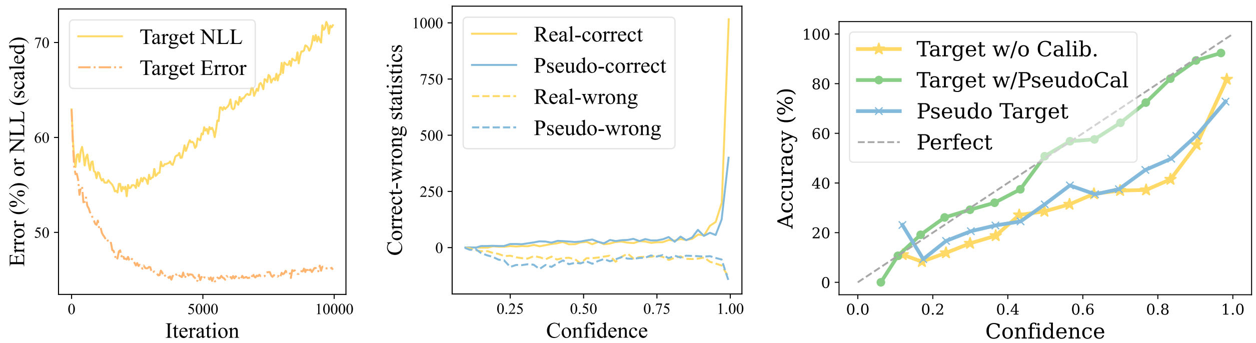

(a) Overfitting of NLL (b) Correct-wrong statistics (c) Reliability diagrams

Figure 1: ATDOC (Liang et al., 2021) on a closed-set UDA task Ar → Cl. (a) illustrates the target error and target NLL loss (rescaled to match error) during UDA training. (b) divides confidence values into 50 bins, displaying the count of correct and wrong predictions in each bin. For real target data, correctness is determined by comparing predictions with ground truths, and for pseudo-target data, it's assessed by comparing predictions with synthesized labels. (c) shows reliability diagrams (Guo et al., 2017) for both pseudo and real target data. Perfect: ideal predictions with no calibration error.

severe *covariate shift* and other distribution shifts, such as label shift (Park et al., 2020). Secondly, despite being based on the simple and post-hoc *temperature scaling*, all of these approaches require additional model training for accurate density estimation, adding complexity. Lastly, these methods rely on labeled source data, which limits their applicability in privacy-preserving UDA scenarios like the recent source-free UDA settings (Liang et al., 2020a; 2022).

In contrast, we adopt a novel perspective, treating UDA calibration as an unsupervised calibration problem in the target domain, which allows us to focus solely on the first challenge. We first study the 'Oracle' case of using labeled target data for *temperature scaling* and then factorize its NLL objective into a joint optimization involving both correct and wrong predictions. This factorization uncovers a key insight with *temperature scaling*: datasets with similar correct-wrong statistics should share similar temperatures. We then introduce a novel post-hoc calibration framework called Pseudo-Calibration (PseudoCal). Concretely, PseudoCal utilizes *mixup* (Zhang et al., 2018) during the inference stage with unlabeled target data to generate a labeled pseudo-target set. It then performs supervised calibration on this labeled set for the temperature. PseudoCal's effectiveness depends on the presence of similar correct-wrong statistics between pseudo and real target data sets. Our intuitive analysis, following the *cluster assumption* (Grandvalet & Bengio, 2004), supports sample-level correspondence between the two datasets. Specifically, pseudo-target samples with correct predictions correspond to correct real target samples, and vice versa, as shown in Figure 1(b). Benefiting from such a high resemblance, PseudoCal significantly improves the calibration performance, as demonstrated in Figure 1(c).

We make three key contributions: *1)* We address the UDA calibration problem from a novel target-domain perspective, for the first time enabling a unified approach across diverse UDA scenarios, including those with label shift or limited source access. *2)* We propose a novel and versatile calibration framework, PseudoCal, which only requires unlabeled target data and a fixed UDA model. PseudoCal synthesizes a labeled pseudo-target set with similar correct-wrong statistics to real target data, successfully converting the challenging unsupervised calibration problem into a readily solvable supervised one. *3)* We conduct a comprehensive evaluation of PseudoCal, involving 5 calibration baselines, to calibrate 10 UDA methods across 5 UDA scenarios. Experimental results demonstrate the superior performance of PseudoCal over all other calibration methods.

2. Related Work

Unsupervised domain adaptation (UDA) has been extensively studied in image classification. Mainstream methods can be categorized into two lines: *1)* Distribution alignment across domains with discrepancy measures (Long et al., 2015) or adversarial learning (Ganin & Lempitsky, 2015; Long et al., 2018; Saito et al., 2018), and *2)* Target domain-based learning with self-training (Shu et al., 2018; Liang et al., 2021) or regularizations (Xu et al., 2019; Cui et al., 2020; Jin et al., 2020). Initially, UDA focused on the *covariate shift* problem (Sugiyama et al., 2007) – two domains share similar label and conditional distributions but have different input distributions. This is commonly called closed-set UDA. Then, more settings have arisen, notably addressing label shift (Lipton et al., 2018). These include partial-set UDA (Cao et al., 2018; Liang et al., 2020b), where some source classes are absent in the target domain, and open-set UDA (Panareda Busto & Gall, 2017), where the target includes samples from unknown classes. Recently, source-free UDA settings have become popular, preserving

Table 1: Comparisons of typical methods for predictive uncertainty calibration in UDA.

Calibration method	Covariate shift	Label shift	No harm to accuracy	No extra training	No source data
TempScal-src (Guo et al., 2017)	✗	✗	✓	✓	✗
MC-Dropout (Gal & Ghahramani, 2016)	✓	✓	✗	✓	✓
Ensemble (Lakshminarayanan et al., 2017)	✓	✓	✓	✗	✓
CPCS (Park et al., 2020)	✓	✗	✓	✗	✗
TransCal (Wang et al., 2020)	✓	✗	✓	✗	✗
PseudoCal (Ours)	✓	✓	✓	✓	✓

source privacy: the white-box setting (Li et al., 2020; Liang et al., 2020a) uses the source model for target adaptation and the black-box setting (Zhang et al., 2021; Liang et al., 2022) only employs the source model for inference. Unlike most studies on improving model accuracy, our work aims to improve the estimation of predictive uncertainty in UDA.

Predictive uncertainty calibration was initially stuidied on binary classification tasks (Zadrozny & Elkan, 2001; Platt et al., 1999). (Guo et al., 2017) extends *Platt scaling* (Platt et al., 1999) to multi-class classification and introduces *matrix scaling* (MatrixScal), *vector scaling* (VectorScal), and *temperature scaling* (TempScal). These post-hoc methods require a labeled validation set for calibration. Some other methods address calibration during model training, including *Monte Carlo Dropout* (MC-Dropout)(Gal & Ghahramani, 2016), Ensemble (Lakshminarayanan et al., 2017), and *Stochastic Variational Bayesian Inference* (Blundell et al., 2015; Louizos & Welling, 2017; Wen et al., 2018). However, an evaluation in (Ovadia et al., 2019) reveals that these methods do not maintain calibration performance under dataset shift. There has been growing interest in calibration under distribution shifts (Alexandari et al., 2020; Wang et al., 2020; Park et al., 2020). Some works perturb the labeled source validation set to serve as a domain-generalized target set (Tomani et al., 2021; Salvador et al., 2021; Zou et al., 2023) or employ it for density estimation (Tomani et al., 2023). Some methods (Gong et al., 2021; Yu et al., 2022) utilize multiple source domains to calibrate the unlabeled target domain in UDA. Additionally, some recent training-stage calibration methods employ smoothed labels (Thulasidasan et al., 2019; Liu et al., 2022) or optimize accuracy-uncertainty differentiably (Krishnan & Tickoo, 2020). In this paper, we specifically address the calibration problem in single-source UDA. A vanilla baseline is to apply IID calibration methods such as TempScal with a labeled source validation set, dubbed TempScal-src. Regarding methods considering the domain shifts, the mainstream idea is to utilize *importance weighting* (Cortes et al., 2008) to address calibration under *covariate shift* in UDA, exemplified by CPCS (Park et al., 2020) and TransCal (Wang et al., 2020). Table 1 presents a comprehensive comparison of typical and relevant UDA calibration methods. Notably, PseudoCal stands out due to its simplicity and versatility.

3. Approach

We introduce unsupervised domain adaptation (UDA) with a C-way image classification task. UDA generally involves two domains: a labeled source domain and an unlabeled target domain. The source domain $\mathcal{D}_{\rm s} = \{(x_{\rm s}^i, y_{\rm s}^i)\}_{i=1}^{n_{\rm s}}$ consists of $n_{\rm s}$ images $x_{\rm s}$ with corresponding one-hot labels $y_{\rm s}$, where $x_{\rm s}^i \in \mathcal{X}_{\rm s}$ and $y_{\rm s}^i \in \mathcal{Y}_{\rm s}$. The target domain $\mathcal{D}_{\rm t} = \{x_{\rm t}^i\}_{i=1}^{n_{\rm t}}$ contains unlabeled images $x_{\rm t}$, where $x_{\rm t}^i \in \mathcal{X}_{\rm t}$. The goal is to learn a UDA model ϕ that can predict the unknown ground truth labels $\{y_{\rm t}^i\}_{i=1}^{n_{\rm t}}$ for the target domain, utilizing data from both domains simultaneously (Ganin & Lempitsky, 2015) or sequentially (Liang et al., 2020a).

When feeding an arbitrary sample (x, y) into model ϕ, we can obtain the predicted one-hot label $\hat{y}$ and the corresponding softmax-based confidence $\hat{p}$. Ideally, the confidence should accurately reflect the probability of correctness, expressed as $\mathbb{P}(\hat{y} = y|\hat{p} = p) = p, \ \forall\ p \in [0, 1]$. This perfect calibration, also known as *Perfect*, is impossible to achieve. The widely used metric for evaluating calibration error is the expected calibration error (ECE) (Guo et al., 2017). ECE involves partitioning probability predictions into M bins, with B_m representing the indices of samples in the m-th bin. It calculates the weighted average of the accuracy-confidence difference across all bins: $\mathcal{L}_{\rm ECE} = \sum_{m=1}^{M} \frac{1}{n}|B_m||\mathrm{acc(B_m)} - \mathrm{conf(B_m)}|$. Here, n represents the number of samples, and for the m-th bin, the accuracy is $\mathrm{acc}\ (B_m) = |B_m|^{-1} \sum_{i \in B_m} \mathbb{1}(\hat{y}_i = y_i)$, and the confidence is $\mathrm{conf}\ (B_m) = |B_m|^{-1} \sum_{i \in B_m} \hat{p}_i$. The introduction of more metrics, such as NLL (Goodfellow et al., 2016) and Brier Score (BS) (Brier et al., 1950), is provided in Appendix B for further reference.

3.1. Factorization of Supervised 'Oracle' Calibration

Unlike the prevalent cross-domain *covariate shift* perspective, we view calibration in UDA as an unsupervised calibration problem within the unlabeled target domain. Before tackling this challenging problem, we study an 'Oracle' solution based on supervised *temperature scaling*

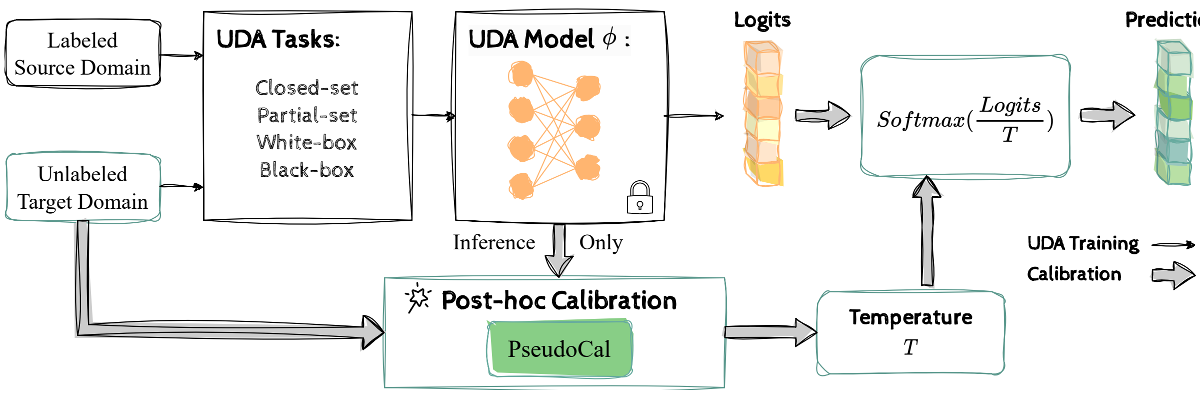

Figure 2: PseudoCal post-hoc calibrates the UDA model's predictive uncertainty in the unlabeled target domain.

(TempScal) (Guo et al., 2017). TempScal is a post-hoc calibration method that optimizes a temperature scalar, denoted as T, on a labeled validation set using the NLL loss between the temperature-flattened softmax predictions and the ground truth labels. For the unlabeled target domain in UDA, we define the calibration achieved by applying TempScal with raw target predictions and unattainable target ground truths as the 'Oracle' calibration. Let z represent the corresponding logit vector for the image input x, and let $\sigma(\cdot)$ denote the softmax function. The 'Oracle' target temperature, denoted as T_o, can be obtained using the original *temperature scaling* optimization: $T_\mathrm{o} = \arg\min_T \mathbb{E}_{(x_\mathrm{t}^i, y_\mathrm{t}^i)\in\mathcal{D}_\mathrm{t}} \mathcal{L}_\mathrm{NLL}\left(\sigma(z_\mathrm{t}^i/T), y_\mathrm{t}^i\right)$.

With further analysis, we observe that target samples can be classified as either being correctly or wrongly predicted when evaluated by target ground truths. Moreover, both types of samples have contrasting effects on the temperature optimization process. Specifically, the NLL minimization favors a small temperature to sharpen the correct predictions and a large temperature to flatten the wrong predictions. Therefore, we can factorize the NLL objective as follows:

$$T_\mathrm{o} = \arg\min_T \frac{N_\mathrm{c}}{N}\mathbb{E}_{(x_\mathrm{t}^i, y_\mathrm{t}^i)\in\mathcal{D}_\mathrm{c}} \mathcal{L}_\mathrm{NLL}\left(\sigma(z_\mathrm{t}^i/T), y_\mathrm{t}^i\right) + \frac{N_\mathrm{w}}{N}\mathbb{E}_{(x_\mathrm{t}^j, y_\mathrm{t}^j)\in\mathcal{D}_\mathrm{w}} \mathcal{L}_\mathrm{NLL}\left(\sigma(z_\mathrm{t}^j/T), y_\mathrm{t}^j\right),$$

where $\mathcal{D}_\mathrm{c}$ represents the set of correctly predicted target samples, comprising N_c instances. Similarly, $\mathcal{D}_\mathrm{w}$ denotes the wrongly predicted set with N_w instances. Obviously, this factorization suggests that when applying TempScal to another labeled set with matching correct-wrong statistics (i.e., the same count of correct and wrong predictions) as the 'Oracle' calibration, the objective of the NLL optimization remains highly consistent, yielding a temperature approximation close to the target oracle temperature T_o.

3.2. Our Unsupervised Solution: Pseudo-Calibration

This straightforward factorization of NLL has inspired effective solutions to calibration in domain generalization using a labeled source validation set (Zou et al., 2023). In contrast, our study focuses specifically on the transductive target domain, leading to the introduction of our novel Pseudo-Calibration (PseudoCal) framework, which operates without utilizing any source data. The main idea is to use the unlabeled target data to synthesize a labeled pseudo-target set that mimics the correct-wrong statistics of the real target set and then apply TempScal to this labeled set.

With only unlabeled target data and a fixed UDA model, the use of predicted labels as pseudo-labels (Lee et al., 2013) is a simple method to generate a labeled set. However, optimizing NLL between raw target predictions and pseudo-labels treats all predictions as correct, ignoring the optimization of wrong predictions in $\mathcal{D}_\mathrm{w}$. This mismatch in correct-wrong statistics can result in poor calibration performance, as demonstrated by 'Pseudo-Label' and 'Filtered-PL' in Table 8. Instead, we employ *mixup* (Zhang et al., 2018) with data across clusters (i.e., with different pseudo-labels), generating mixed samples that inherently include both correct and wrong predictions when evaluated with mixed labels.

Step 1: Pseudo-target synthesis. We generate a pseudo-target set by applying *mixup* to target samples in the inference stage. Specifically, a pseudo-target sample x_pt and its label vector y_pt are obtained by taking a convex combination of a pair of real target samples $x_\mathrm{t}^i, x_\mathrm{t}^j$ from different clusters and their pseudo-labels $\hat{y}_\mathrm{t}^i, \hat{y}_\mathrm{t}^j$. Consequently, we obtain a labeled pseudo-target set $\{(x_\mathrm{pt}^i, y_\mathrm{pt}^i)\}_{i=1}^{n_\mathrm{pt}}$, where n_pt represents the amount. The general formulation is:

$$x_\mathrm{pt} = \lambda * x_\mathrm{t}^i + (1-\lambda) * x_\mathrm{t}^j, \quad y_\mathrm{pt} = \lambda * \hat{y}_\mathrm{t}^i + (1-\lambda) * \hat{y}_\mathrm{t}^j,$$

where $\lambda \in (0.5, 1.0)$ is a fixed scalar used as the mix ratio, different from that in common *mixup*.

Step 2: Supervised calibration. Using the synthesized labeled pseudo-target set $\{(x_{\mathrm{pt}}^i, y_{\mathrm{pt}}^i)\}_{i=1}^{n_{\mathrm{pt}}}$, we can easily determine its optimal pseudo-target temperature through TempScal. This estimated temperature serves as an approximation of the 'Oracle' target temperature T_{o}.

With the above two simple steps, PseudoCal successfully transforms the challenging unsupervised calibration problem associated with the unlabeled real target set into a supervised one with the labeled pseudo-target set and readily solves it with TempScal. The pipeline of PseudoCal is illustrated in Figure 2, where the UDA model is utilized as a black box solely for inferring the predictions of input data. A comprehensive Pytorch-style pseudocode is in Appendix A.

Analysis. Built upon the well-established *cluster assumption* (Grandvalet & Bengio, 2004; Chapelle & Zien, 2005), we intuitively analyze how mixed samples can exhibit similar correct-wrong statistics as real target data, as shown in Figure 1(b). This assumption suggests that within a well-learned data structure, samples located far from the classification boundary are more likely to be correctly classified, while those near the boundary are prone to misclassification. Instead of using this assumption as an objective in model training (Shu et al., 2018; Verma et al., 2022), our focus here is to employ it for explaining the inference behavior of a UDA model ϕ, which often effectively learns the underlying target-domain structure. For simplicity, let's assume all involved labels in *mixup* are one-hot, and consider a fixed mix ratio λ noticeably greater than 0.5. This ensures a clear distinction between two involved real samples: one primary sample x_{t}^i with a mix ratio greater than 0.5, determining the mixed label y_{pt} for the mixed sample x_{pt}, and the other as the minor sample x_{t}^j, serving only as an input perturbation. If x_{pt} yields a correct model prediction $\hat{y}_{\mathrm{pt}}$ evaluated by its mixed label (i.e., $\hat{y}_{\mathrm{pt}} == y_{\mathrm{pt}}$), it suggests that the real sample x_{t}^i maintains its prediction after cross-cluster perturbation. This implies that x_{t}^i is likely distant from the classification boundary, and its prediction or pseudo-label $\hat{y}_{\mathrm{t}}^i$ is genuinely correct when evaluated against its ground truth y_{t}^i. Similar analysis can be easily applied to x_{pt} with a wrong prediction $\hat{y}_{\mathrm{pt}}$ (i.e., $\hat{y}_{\mathrm{pt}} \neq y_{\mathrm{pt}}$).The presence of sample-level correspondence, when observed at the dataset level, manifests as similar correct-wrong statistics. However, this correspondence may not hold under extreme perturbation degrees (i.e., λ quite near 0.5 or 1.0). Kindly refer to Appendix D for detailed empirical evidence.

4. Experiments

4.1. Settings

Datasets. For image classification, we adopt 5 popular UDA benchmarks of varied scales. *Office-31* (Saenko et al., 2010) is a small-scale benchmark with 31 classes in 3 domains: Amazon (A), DSLR (D), and Webcam (W). *Office-Home* (Venkateswara et al., 2017) is a medium-scale benchmark with 65 classes in 4 domains: Art (Ar), Clipart (Cl), Product (Pr), and Real-World (Re). *VisDA* (Peng et al., 2017) is a large-scale benchmark with over 200k images across 12 classes in 2 domains: Training (T) and Validation (V). *DomainNet* (Peng et al., 2019) is a large-scale benchmark with 600k images. We take a subset of 126 classes with 7 tasks(Saito et al., 2019) from 4 domains: Real (R), Clipart (C), Painting (P), and Sketch (S). *Image-Sketch* (Wang et al., 2019) is a large-scale benchmark with 1000 classes in 2 domains: ImageNet (I) and Sketch (S). For semantic segmentation, we use *Cityscapes*(Cordts et al., 2016) as the target domain and either *GTA5*(Richter et al., 2016) or *SYNTHIA* (Ros et al., 2016) as the source.

UDA methods. We evaluate calibration on 10 UDA methods across 5 UDA scenarios. For image classification, we cover closed-set UDA methods (ATDOC (Liang et al., 2021), BNM (Cui et al., 2020), MCC (Jin et al., 2020), CDAN (Long et al., 2018), SAFN (Xu et al., 2019), MCD (Saito et al., 2018)), partial-set UDA methods (ATDOC (Liang et al., 2021), MCC (Jin et al., 2020), PADA (Cao et al., 2018)), the whit-box source-free UDA method (SHOT (Liang et al., 2020a)), and the black-box source-free UDA method (DINE (Liang et al., 2022)). For semantic segmentation, we focus on calibrating source-only models without applying domain adaptation techniques.

Calibration baselines. For a comprehensive comparison, we consider 5 typical calibration baselines in UDA, as compared in Table 1, including the no calibration baseline (No Calib.), source-domain calibration (TempScal-src), cross-domain calibration (CPCS, TransCal), and another versatile unsupervised calibration method (Ensemble).

Implementation details. We train all UDA models using their official code until convergence on an RTX TITAN GPU. We adopt ResNet-101 (He et al., 2016) for *VisDA* and segmentation tasks, ResNet-34 for *DomainNet*, and ResNet-50 for all other tasks. For PseudoCal, a fixed mix ratio λ of 0.65 is employed in all experiments. The UDA model is fixed for only inference use. We use it for one-epoch inference with *mixup* to generate the labeled pseudo-target set. The reported results are averaged over five random runs.

4.2. Results

We evaluate PseudoCal across 5 UDA scenarios. For classification, we report the averaged ECE across UDA tasks sharing the same target domain in Tables 2-6. For segmentation, we take each pixel as a sample and report the results in Table 7. 'Oracle' refers to the 'Oracle' calibration with the target domain ground truths. 'Accuracy' (%) denotes the target domain accuracy of the fixed UDA model. Refer to Appendix C for segmentation details and Appendix E for full results, including ECE results for each UDA task.

Table 2: ECE (%) of closed-set UDA on *Office-Home* (*Home*). Lower is better. **bold**: Best case.

Method	ATDOC					BNM					MCC				
	→Ar	→Cl	→Pr	→Re	avg	→Ar	→Cl	→Pr	→Re	avg	→Ar	→Cl	→Pr	→Re	avg
No Calib.	10.07	22.35	8.61	6.06	11.77	30.97	39.85	19.70	16.73	26.81	13.25	23.11	12.33	10.53	14.81
TempScal-src	6.19	17.54	**3.98**	**3.03**	7.68	23.11	30.32	13.70	10.25	19.35	6.74	16.25	**5.08**	4.10	8.04
CPCS	14.13	14.75	11.02	7.33	11.81	24.76	25.02	14.90	8.80	18.37	19.11	28.59	14.65	5.55	16.97
TransCal	18.09	6.52	16.03	18.29	14.73	17.44	27.22	9.14	5.47	14.82	11.73	3.86	6.70	8.16	7.61
Ensemble	7.38	18.01	5.51	4.22	8.78	22.50	30.68	14.38	12.53	20.02	9.76	19.20	9.48	7.90	11.58
PseudoCal (ours)	**2.42**	**2.93**	5.84	5.07	**4.07**	**17.34**	**16.03**	**6.20**	**4.68**	**11.06**	**2.85**	**2.25**	5.18	**3.57**	**3.47**
Oracle	1.71	1.91	2.29	1.69	1.90	2.20	2.53	2.36	1.60	2.17	2.25	1.64	2.22	1.91	2.00
Accuracy (%)	66.42	52.39	76.60	77.74	68.29	65.42	53.69	76.51	78.98	68.65	61.03	47.47	72.37	74.03	63.73

Method	CDAN					SAFN					MCD					*Home*
	→Ar	→Cl	→Pr	→Re	avg	→Ar	→Cl	→Pr	→Re	avg	→Ar	→Cl	→Pr	→Re	avg	AVG
No Calib.	13.38	22.94	12.15	10.00	14.62	16.57	27.90	13.16	11.93	17.39	16.36	25.96	13.29	11.97	16.89	17.05
TempScal-src	6.89	15.44	5.01	4.19	7.88	6.99	16.13	4.56	**4.07**	7.94	6.01	12.15	**3.56**	**3.54**	6.31	9.53
CPCS	18.38	33.56	15.29	9.90	19.28	14.98	30.54	10.06	12.11	16.92	25.13	27.26	10.17	14.29	19.21	17.09
TransCal	14.76	4.72	12.07	13.73	11.32	3.50	6.87	**3.77**	4.15	4.57	10.78	**2.66**	10.31	11.27	8.76	10.30
Ensemble	10.07	18.58	9.15	7.23	11.26	14.82	24.90	11.17	9.86	15.19	12.36	20.87	8.93	7.64	12.45	13.21
PseudoCal (ours)	**5.10**	**3.72**	**4.71**	**2.40**	**3.98**	**3.05**	**3.34**	6.86	4.37	**4.41**	**4.07**	2.86	6.26	3.72	**4.23**	**5.20**
Oracle	3.61	2.84	2.26	1.94	2.66	1.96	2.48	2.52	1.74	2.17	2.65	2.27	2.30	2.22	2.36	2.21
Accuracy (%)	62.26	49.99	71.19	73.79	64.31	65.84	51.90	73.78	75.09	66.66	59.04	46.80	68.75	71.39	61.49	65.52

Table 3: ECE (%) of closed-set UDA on *Office-31* (*Office*) and *VisDA*.

Method	ATDOC					BNM					MCC				
	→A	→D	→W	avg	T→V	→A	→D	→W	avg	T→V	→A	→D	→W	avg	T→V
No Calib.	12.17	4.59	6.66	7.81	10.38	23.41	11.12	8.27	14.27	17.10	19.29	6.18	7.80	11.09	17.42
TempScal-src	22.39	**3.39**	4.18	9.99	10.53	23.85	9.23	4.98	12.69	13.72	21.38	3.79	3.00	9.39	13.28
CPCS	24.64	7.98	8.94	13.85	16.65	22.45	11.65	**2.02**	12.04	15.36	30.16	4.69	3.03	12.63	7.14
TransCal	12.14	14.21	14.64	13.67	6.36	14.86	**5.22**	2.70	7.59	8.79	6.53	3.77	3.91	4.74	12.21
Ensemble	9.79	3.60	**4.09**	5.83	8.53	19.77	6.92	4.63	10.44	14.84	17.48	3.07	4.88	8.48	15.32
PseudoCal (ours)	**3.85**	6.64	4.98	**5.16**	**5.27**	**9.48**	6.30	3.97	**6.58**	**3.03**	**4.61**	**2.68**	**2.82**	**3.37**	**1.20**
Oracle	2.13	2.49	3.15	2.59	0.52	2.52	2.65	1.40	2.19	0.93	2.24	2.36	2.67	2.42	1.12
Accuracy (%)	73.23	91.57	88.93	84.58	75.96	72.56	88.35	90.94	83.95	76.23	69.69	91.37	89.06	83.37	78.00

Method	CDAN					SAFN					MCD					*Office*	*VisDA*
	→A	→D	→W	avg	T→V	→A	→D	→W	avg	T→V	→A	→D	→W	avg	T→V	AVG	AVG
No Calib.	17.02	9.34	7.96	11.44	15.90	21.34	6.17	6.68	11.40	18.53	16.71	9.49	8.88	11.69	17.58	11.28	16.15
TempScal-src	18.54	5.70	3.41	9.21	14.19	23.95	3.21	2.83	9.99	14.40	25.37	**3.44**	**2.36**	10.39	10.22	10.28	12.72
CPCS	17.47	30.95	5.67	18.03	15.45	23.15	8.21	18.21	16.52	17.88	27.69	11.85	19.01	19.52	10.56	15.43	13.84
TransCal	**4.84**	7.44	6.84	6.38	4.07	8.14	**3.04**	2.81	**4.67**	8.23	5.13	5.65	4.76	5.18	**3.74**	7.04	7.23
Ensemble	10.92	4.98	3.29	6.40	13.30	18.89	3.81	5.75	9.48	17.31	14.56	6.25	5.49	8.77	14.82	8.23	14.02
PseudoCal (ours)	6.58	**4.78**	**3.04**	**4.80**	**3.04**	**4.13**	7.92	5.51	5.85	**7.54**	**4.22**	5.97	5.33	**5.17**	6.71	**5.16**	**4.46**
Oracle	3.21	3.26	2.17	2.88	1.00	2.21	2.90	1.75	2.29	1.82	2.11	3.55	1.76	2.47	0.99	2.47	1.06
Accuracy (%)	66.03	87.15	87.17	80.12	75.24	68.95	89.96	88.55	82.49	73.91	67.07	86.14	85.53	79.58	72.18	82.35	75.25

Closed-set UDA. We evaluate 6 UDA methods on 4 benchmarks for closed-set UDA. We report the ECE for *Office-Home* in Table 2, ECE for both *Office-31* and *VisDA* in Table 3, and ECE for *DomainNet* in Table 4. PseudoCal consistently achieves a low ECE close to 'Oracle', significantly outperforming other calibration methods by a large margin. On the evaluated benchmarks, PseudoCal shows average ECE improvements of 4.33% on *Office-Home*, 1.88% on *Office-31*, 2.77% on *VisDA*, and 5.95% on *DomainNet* when compared to the second-best calibration method.

Partial-set UDA. We evaluate 3 partial-set UDA methods on *Office-Home* and report the ECE in Table 5. PseudoCal consistently performs the best on average and outperforms the second-best method (Ensemble) by a margin of 4.24%.

Source-free UDA. We evaluate source-free UDA settings using SHOT and DINE. We report the ECE for *DomainNet* and *Image-Sketch* together in Table 6. PseudoCal outperforms Ensemble on both benchmarks by significant margins, with 7.44% on *DomainNet* and 15.05% on *Image-Sketch*.

Semantic segmentation. In addition to various classification tasks, we also evaluate PseudoCal on the domain adaptive semantic segmentation tasks and report the ECE in Table 7. Remarkably, PseudoCal performs the best on average and demonstrates an average ECE improvement of 4.62% over the no-calibration baseline.

4.3. Discussion

Qualitative comparisons. Reliability diagrams in Figure 3(a) show that PseudoCal aligns with 'Oracle', while the state-of-the-art method TransCal deviates significantly.

Table 4: ECE (%) of closed-set UDA on *DomainNet* (*DNet*).

Method	ATDOC					BNM					MCC					*DNet*
	→C	→P	→R	→S	avg	→C	→P	→R	→S	avg	→C	→P	→R	→S	avg	AVG
No Calib.	9.54	7.38	3.75	12.29	8.24	28.57	22.10	15.37	31.27	24.33	8.63	7.77	4.79	13.61	8.70	
TempScal-src	8.69	7.71	1.94	11.82	7.54	19.04	13.62	9.40	20.30	15.59	8.38	8.32	**2.36**	13.88	8.23	
CPCS	10.78	4.72	4.46	13.38	8.34	8.23	7.92	7.98	9.29	8.36	9.03	4.33	3.44	17.21	8.50	
TransCal	23.02	24.76	26.65	19.68	23.52	**6.52**	**1.84**	**5.82**	9.39	**5.89**	22.27	24.06	23.45	18.03	21.95	
Ensemble	6.32	4.54	**1.59**	9.05	5.37	23.44	18.61	12.61	26.21	20.22	5.71	5.10	2.57	10.34	5.93	
PseudoCal (ours)	**1.82**	**1.41**	2.51	**1.70**	**1.86**	10.27	6.01	6.18	**5.86**	7.08	**1.35**	**1.89**	2.38	**3.10**	**2.18**	
Oracle	1.55	0.94	0.86	1.07	1.10	2.40	1.66	3.40	1.30	2.19	1.16	1.44	1.09	0.89	1.14	
Accuracy (%)	56.05	60.64	74.95	52.08	60.93	56.62	63.13	74.30	52.25	61.57	50.89	57.74	71.62	46.39	56.66	
Method	CDAN					SAFN					MCD					*DNet*
	→C	→P	→R	→S	avg	→C	→P	→R	→S	avg	→C	→P	→R	→S	avg	AVG
No Calib.	10.17	9.64	5.56	14.44	9.95	17.94	14.44	10.15	21.26	15.95	9.56	7.40	3.80	12.93	8.42	12.60
TempScal-src	7.92	8.31	2.75	12.30	7.82	9.61	8.15	4.12	14.18	9.02	6.48	6.96	4.06	11.20	7.18	9.23
CPCS	10.75	4.28	5.57	6.91	6.88	10.92	5.91	8.22	22.59	11.91	7.02	3.51	1.96	21.79	8.57	8.76
TransCal	20.92	21.41	22.93	16.93	20.55	10.75	12.88	14.28	6.88	11.20	21.48	24.99	27.45	18.95	23.22	17.72
Ensemble	7.21	6.74	3.54	11.29	7.20	16.59	13.25	9.08	19.52	14.61	7.25	5.27	2.86	11.34	6.68	10.00
PseudoCal (ours)	**1.58**	**1.89**	**1.86**	**2.67**	**2.00**	**3.33**	**1.30**	**1.50**	**2.76**	**2.22**	**2.27**	**1.16**	**1.01**	**1.70**	**1.53**	**2.81**
Oracle	1.45	1.08	1.07	0.94	1.13	1.43	0.92	1.21	0.72	1.07	1.33	0.97	0.56	0.68	0.88	1.25
Accuracy (%)	53.11	59.13	71.82	49.09	58.29	49.59	58.03	66.40	47.66	55.42	48.85	57.99	65.32	47.95	55.03	57.98

Table 5: ECE (%) of partial-set UDA on *Office-Home* (*Home*).

Method	ATDOC					MCC					PADA					*Home*
	→Ar	→Cl	→Pr	→Re	avg	→Ar	→Cl	→Pr	→Re	avg	→Ar	→Cl	→Pr	→Re	avg	AVG
No Calib.	16.68	28.47	20.00	12.26	19.35	12.71	22.17	12.21	8.99	14.02	9.45	19.09	9.19	6.77	11.13	14.83
TempScal-src	13.40	24.79	14.91	8.72	15.45	7.12	15.97	6.04	**4.35**	8.37	8.92	18.20	6.21	4.08	9.35	11.06
CPCS	19.39	29.74	13.86	14.63	19.41	12.73	28.11	9.09	10.69	15.16	24.40	22.74	17.30	27.67	23.03	19.20
TransCal	10.64	**5.17**	**5.88**	11.30	8.25	9.44	4.27	**5.41**	6.98	6.53	22.70	11.00	23.00	26.77	20.87	11.88
Ensemble	11.98	21.28	13.44	8.62	13.83	9.22	18.54	10.11	6.78	11.16	5.30	11.86	**4.43**	**3.92**	**6.38**	10.46
PseudoCal (ours)	**7.87**	10.90	6.24	**4.83**	**7.46**	**3.74**	**3.63**	6.93	4.81	**4.78**	**4.72**	**3.45**	10.77	6.69	6.41	**6.22**
Oracle	4.13	4.45	4.37	4.08	4.26	2.81	3.01	3.06	2.37	2.81	3.94	2.65	4.80	3.03	3.61	3.56
Accuracy (%)	63.02	50.70	65.92	73.71	63.34	65.53	51.68	73.41	78.23	67.21	55.65	44.06	61.23	66.54	56.87	62.47

Table 6: ECE (%) of source-free UDA on *DomainNet* (*DNet*) and *ImageNet-Sketch* (*Sketch*).

Method	SHOT						DINE						*DNet*	*Sketch*
	→C	→P	→R	→S	avg	I→S	→C	→P	→R	→S	avg	I→S	AVG	AVG
No Calib.	17.16	21.19	10.03	23.14	17.88	34.71	21.99	22.51	12.39	30.34	21.81	58.85	19.84	46.78
Ensemble	14.24	17.94	7.81	19.49	14.87	33.03	17.88	18.86	10.83	25.33	18.22	53.24	16.54	43.14
PseudoCal (ours)	**6.66**	**7.78**	**2.91**	**6.67**	**6.00**	**8.42**	**14.42**	**12.95**	**5.30**	**16.15**	**12.20**	**47.76**	**9.10**	**28.09**
Oracle	3.27	2.52	1.37	2.18	2.33	4.39	1.75	1.80	1.29	1.37	1.55	5.90	1.94	5.14
Accuracy (%)	66.52	64.48	78.34	59.64	67.25	34.29	63.76	65.47	80.69	55.51	66.36	22.27	66.80	28.28

Table 7: ECE (%) of segmentation.

Method	*GTA5*	*SYNTHIA*	AVG
No Calib.	7.87	23.08	15.48
TempScal-src	4.61	19.24	11.93
Ensemble	**2.66**	20.84	11.75
PseudoCal (ours)	5.73	**15.99**	**10.86**
Oracle	0.52	4.50	2.51

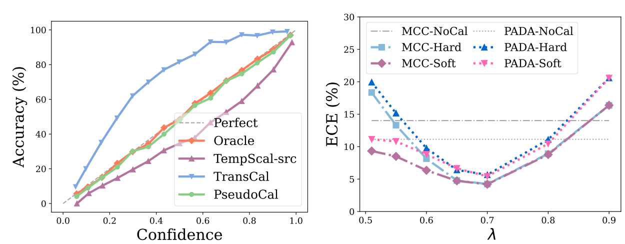

(a) CDAN on R → S (b) Partial-set UDA on *Home*

Figure 3: (a) provides the reliability diagrams. (b) presents the sensitivity analysis of the fixed mix ratio λ.

Impact of mix ratio λ. The fixed mix ratio λ is the sole hyperparameter in PseudoCal. We investigate its impact on calibration performance by experimenting with values ranging from 0.51 to 0.9. Results of two typical UDA methods for partial-set tasks on *Office-Home* are shown in Figure 3(b). We first examine *mixup* with both 'Hard' (one-hot labels) and 'Soft' (soft probability predictions) labels, finding similar trends with differences that are generally not visible when $\lambda > 0.6$. In addition, optimal performance for Pseu-

Table 8: ECE (%) of ablation experiments on pseudo-target synthesis.

Method	MCD		BNM		CDAN	SHOT	PADA		DINE
	D→A	W→A	Cl→Pr	Pr→Re	R→C	I→S	Ar→Cl	Re→Ar	P→R
No Calib.	16.39	17.03	22.09	15.72	9.83	34.71	20.35	8.31	12.39
MocoV2Aug (Chen et al., 2020)	16.85	17.21	20.51	14.98	15.49	28.63	25.81	15.17	11.12
RandAug (Cubuk et al., 2020)	12.87	11.53	19.24	11.37	13.33	29.28	18.47	10.32	12.62
CutMix (Yun et al., 2019)	8.20	6.39	14.82	10.60	7.60	23.18	15.96	6.04	6.93
ManifoldMix (Verma et al., 2019)	19.49	19.27	23.29	16.94	27.00	50.54	36.04	21.29	16.88
Mixup-Beta (Zhang et al., 2018)	14.96	13.11	15.65	11.24	15.84	26.74	23.85	11.46	9.72
Pseudo-Label (Lee et al., 2013)	32.47	33.35	26.31	19.65	47.02	65.70	56.18	36.27	19.31
Filtered-PL (Sohn et al., 2020)	31.74	32.73	26.14	19.46	45.35	64.29	54.83	35.10	19.05
PseudoCal-same	19.31	20.54	22.50	15.63	25.43	45.54	30.30	18.46	15.56
PseudoCal (ours)	**4.38**	**4.06**	**6.31**	**4.76**	**1.51**	**8.42**	**2.95**	**3.71**	**5.29**
Oracle	2.31	1.90	3.14	1.10	1.28	4.39	2.16	2.87	1.29
Accuracy (%)	67.52	66.63	73.69	80.35	52.98	34.29	43.82	63.73	80.69

doCal occurs with a moderate λ value between 0.6 and 0.8. The reason is that a λ value closer to 0.5 generates more ambiguous samples, resulting in increased wrong predictions, whereas a λ value closer to 1.0 has the opposite effect. More evidence is in Appendix D, where we examine the impact of λ on sample-level correspondence. At last, for simplicity, we use a fixed λ value of 0.65 with one-hot labels for all experiments.

Table 9: ViT results of MCC on C→S.

Method	ECE (%)	BS	NLL
No Calib.	11.52	0.5674	1.9592
TempScal-src	10.63	0.5647	1.9418
CPCS	5.48	0.5579	1.8781
TransCal	23.38	0.6279	2.1089
Ensemble	10.08	0.5618	1.9260
PseudoCal (ours)	**3.63**	**0.5553**	**1.8697**
Oracle	1.29	0.5519	1.8597

Impact of backbones and metrics. To examine the robustness of PseudoCal across different backbones and calibration metrics, we assess its performance using ViT-B (Dosovitskiy et al., 2021) as the backbone and present the results for the aforementioned three metrics in Table 9. The findings reveal that PseudoCal consistently achieves the best performance with different backbones or calibration metrics.

Table 10: ECE (%) of model calibration at different iterations (batch size: 36) during the training of the ATDOC model shown in Figure 1(a).

Method	1	5	10	50	100	500	1000
No Calib.	**21.51**	**11.11**	**7.71**	11.74	16.38	21.48	22.28
PseudoCal (ours)	73.91	46.06	34.91	**6.01**	**4.43**	**2.87**	**3.67**
Oracle	0.00	1.77	0.84	1.78	2.31	2.16	1.89
Accuracy (%)	1.97	4.28	11.25	37.25	40.64	45.73	49.00

Impact of UDA model quality. We provide the target-domain accuracy for each model in the 'Accuracy' row. PseudoCal remains effective as long as the model has learned some target structure instead of being completely randomly initialized, supported by *cluster assumption*. This effectiveness is evident in Table 6, where PseudoCal maintains its competence even with low accuracy pseudo-labels (around 30%). Additionally, we examine the influence of model (pseudo-label) quality on calibration results throughout UDA training, with results presented in Table 10. If the model quality is particularly low, for instance, with an accuracy below 15%, PseudoCal becomes ineffective. Fortunately, PseudoCal operates as a post-hoc method, which allows it to function effectively once the UDA model has been adequately trained.

Comparison with training-stage *mixup*. Most approaches incorporate *mixup* (Zhang et al., 2018) during the model training stage as an objective to enhance model generalization, and among them, (Thulasidasan et al., 2019) further utilizes *mixup* as a training-stage calibration method. However, our use of *mixup* in PseudoCal differs significantly from previous *mixup*-based works in three key aspects. *1)* Different stage: All of these works apply *mixup* in training, while our *mixup* operation occurs in the inference stage to synthesize a labeled set. *2)* Different mix ratio: PseudoCal leverages *mixup* for cross-cluster sample interpolation and performs effectively with a fixed mix ratio $\lambda \in (0.6, 0.8)$ but is considerably less effective with λ values close to 1.0. In contrast, previous methods typically work best with $\lambda \in \text{Beta}(\alpha, \alpha)$ where $\alpha \in [0.1, 0.4]$, essentially favoring λ values that are close to 1.0. However, they are ineffective with λ values close to 0.5 (like our adopted values) due to the manifold intrusion problem (Thulasidasan et al., 2019; Guo et al., 2019). *3)* Different performance: We observed that UDA models trained with training-time calibration methods still suffer from significant miscalibration, while our PseudoCal can further substantially reduce ECE errors for these models. For example, as shown in Table 6, SHOT employs *label smoothing* for training (Liu et al., 2022), and DINE is trained with *mixup* (Thulasidasan et al., 2019).

Ablation study on pseudo-target synthesis. Pseudo-target synthesis plays a critical role in our PseudoCal framework. In this step, we employ input-level *mixup* with a fixed mix ratio (λ) to generate a pseudo-target sample by combining two real samples with different pseudo-labels. We conduct a comprehensive ablation study on this synthesis strategy by comparing it with alternative approaches, including: *1)* Applying *mixup* between samples with the same pseudo-label (referred to as PseudoCal-same). *2)* Using instance-based augmentations of target samples, such as RandAugment (Cubuk et al., 2020), and strong augmentations commonly used in self-supervised learning (Chen et al., 2020). *3)* Employing *mixup* at different levels, such as the patch-level (Yun et al., 2019) and the feature-level (Verma et al., 2019). *4)* Applying common training-stage *mixup* using $\lambda \in \text{Beta}(0.3, 0.3)$ (Zhang et al., 2018). *5)* Directly utilizing original or filtered pseudo-labeled real target samples (Lee et al., 2013; Sohn et al., 2020) without *mixup* (by setting λ to 1.0). We present an extensive comparison of all these strategies in Table 8. The results consistently demonstrate that our inference-stage input-level *mixup* outperforms the alternative options.

Limitation discussion. PseudoCal has the following limitations: *1)* Like all of the existing calibration methods compared, PseudoCal may occasionally increase ECE when the initial ECE is already small (see $\rightarrow$D in Table 3). This is acceptable considering that unsupervised calibration remains an open problem. *2)* PseudoCal may face challenges in extreme cases with very few available unlabeled target samples, such as only a small batch of samples or even a single target sample. *3)* PseudoCal is partly dependent on the *cluster assumption*, and it may fail if the target pseudo label is extremely poor, i.e., performing similarly to random trials. Regarding the last two limitations, similarly, all of the existing UDA calibration methods would fail under these extreme situations. In general, as we illustrate in Table 1, our PseudoCal has fewer limitations compared with existing prevalent UDA calibration solutions.

5. Conclusion

In conclusion, we introduce PseudoCal, a novel and versatile post-hoc framework for calibrating predictive uncertainty in unsupervised domain adaptation (UDA). By focusing on the unlabeled target domain, PseudoCal distinguishes itself from mainstream calibration methods that are based on *covariate shift* and eliminates their associated limitations. To elaborate, PseudoCal employs a novel inference-stage *mixup* strategy to synthesize a labeled pseudo-target set that mimics the correct-wrong statistics in real target samples. In this way, PseudoCal successfully transforms the challenging unsupervised calibration problem involving unlabeled real samples into a supervised one using labeled pseudo-target data, which can be readily addressed through *temperature scaling*. Throughout our extensive evaluations spanning diverse UDA settings, including source-free UDA settings and domain adaptive semantic segmentation, PseudoCal consistently showcases its advantages of simplicity, versatility, and effectiveness in enhancing calibration in UDA. In future work, we aim to extend PseudoCal to additional practical UDA scenarios, including open-set UDA.

Acknowledgements

The authors would like to thank the anonymous reviewers for their valuable comments. Jian Liang is supported by the Beijing Nova Program under Grant Z211100002121108 and the National Natural Science Foundation of China (Grant No. 62276256). Xinchao Wang is supported by the Singapore Ministry of Education Academic Research Fund Tier 1 (WBS: A-8001229-00-00), a project titled "Towards Robust Single Domain Generalization in Deep Learning".

Impact Statement

This paper advances the subfield of machine learning by addressing the unsupervised calibration problem in transductive learning. While our work has numerous potential societal implications, we choose not to highlight specific ones here. The main potential negative impact is that in safety-critical decision-making scenarios, such as autonomous driving and medical diagnosis, the proposed method may occasionally increase calibration error if the original calibration error is already small.

References

Alexandari, A., Kundaje, A., and Shrikumar, A. Maximum likelihood with bias-corrected calibration is hard-to-beat at label shift adaptation. In *International Conference on Machine Learning*, 2020.

Blundell, C., Cornebise, J., Kavukcuoglu, K., and Wierstra, D. Weight uncertainty in neural network. In *International Conference on Machine Learning*, 2015.

Brier, G. W. et al. Verification of forecasts expressed in terms of probability. *Monthly Weather Review*, 78(1):1–3, 1950.

Bucci, S., Loghmani, M. R., and Tommasi, T. On the effectiveness of image rotation for open set domain adaptation. In *European Conference on Computer Vision*, 2020.

Cao, Z., Ma, L., Long, M., and Wang, J. Partial adversarial domain adaptation. In *European Conference on Computer Vision*, 2018.

Chapelle, O. and Zien, A. Semi-supervised classification by low density separation. In *International Workshop on Artificial Intelligence and Statistics*, 2005.

Chen, X., Fan, H., Girshick, R., and He, K. Improved baselines with momentum contrastive learning. *arXiv preprint arXiv:2003.04297*, 2020.

Cordts, M., Omran, M., Ramos, S., Rehfeld, T., Enzweiler, M., Benenson, R., Franke, U., Roth, S., and Schiele, B. The cityscapes dataset for semantic urban scene understanding. In *IEEE Conference on Computer Vision and Pattern Recognition*, 2016.

Cortes, C., Mohri, M., Riley, M., and Rostamizadeh, A. Sample selection bias correction theory. In *Algorithmic Learning Theory*, 2008.

Cubuk, E. D., Zoph, B., Shlens, J., and Le, Q. V. Randaugment: Practical automated data augmentation with a reduced search space. In *IEEE Conference on Computer Vision and Pattern Recognition, Workshops*, 2020.

Cui, S., Wang, S., Zhuo, J., Li, L., Huang, Q., and Tian, Q. Towards discriminability and diversity: Batch nuclear-norm maximization under label insufficient situations. In *IEEE Conference on Computer Vision and Pattern Recognition*, 2020.

de Jorge, P., Volpi, R., Torr, P., and Rogez, G. Reliability in semantic segmentation: Are we on the right track? *arXiv preprint arXiv:2303.11298*, 2023.

Dosovitskiy, A., Beyer, L., Kolesnikov, A., Weissenborn, D., Zhai, X., Unterthiner, T., Dehghani, M., Minderer, M., Heigold, G., Gelly, S., et al. An image is worth 16x16 words: Transformers for image recognition at scale. In *International Conference on Learning Representations*, 2021.

Fu, B., Cao, Z., Long, M., and Wang, J. Learning to detect open classes for universal domain adaptation. In *European Conference on Computer Vision*, 2020.

Gal, Y. and Ghahramani, Z. Dropout as a bayesian approximation: Representing model uncertainty in deep learning. In *International Conference on Machine Learning*, 2016.

Ganin, Y. and Lempitsky, V. Unsupervised domain adaptation by backpropagation. In *International Conference on Machine Learning*, 2015.

Gong, Y., Lin, X., Yao, Y., Dietterich, T. G., Divakaran, A., and Gervasio, M. Confidence calibration for domain generalization under covariate shift. In *IEEE International Conference on Computer Vision*, 2021.

Goodfellow, I., Bengio, Y., and Courville, A. *Deep learning*. MIT press, 2016.

Grandvalet, Y. and Bengio, Y. Semi-supervised learning by entropy minimization. In *Advances in Neural Information Processing Systems*, 2004.

Guo, C., Pleiss, G., Sun, Y., and Weinberger, K. Q. On calibration of modern neural networks. In *International Conference on Machine Learning*, 2017.

Guo, H., Mao, Y., and Zhang, R. Mixup as locally linear out-of-manifold regularization. In *AAAI Conference on Artificial Intelligence*, 2019.

He, K., Zhang, X., Ren, S., and Sun, J. Deep residual learning for image recognition. In *IEEE Conference on Computer Vision and Pattern Recognition*, 2016.

Jin, Y., Wang, X., Long, M., and Wang, J. Minimum class confusion for versatile domain adaptation. In *European Conference on Computer Vision*, 2020.

Krishnan, R. and Tickoo, O. Improving model calibration with accuracy versus uncertainty optimization. In *Advances in Neural Information Processing Systems*, 2020.

Lakshminarayanan, B., Pritzel, A., and Blundell, C. Simple and scalable predictive uncertainty estimation using deep ensembles. In *Advances in Neural Information Processing Systems*, 2017.

Lee, D.-H. et al. Pseudo-label: The simple and efficient semi-supervised learning method for deep neural networks. In *International Conference on Machine Learning, Workshop*, 2013.

Li, R., Jiao, Q., Cao, W., Wong, H.-S., and Wu, S. Model adaptation: Unsupervised domain adaptation without source data. In *IEEE Conference on Computer Vision and Pattern Recognition*, 2020.

Liang, J., Hu, D., and Feng, J. Do we really need to access the source data? source hypothesis transfer for unsupervised domain adaptation. In *International Conference on Machine Learning*, 2020a.

Liang, J., Wang, Y., Hu, D., He, R., and Feng, J. A balanced and uncertainty-aware approach for partial domain adaptation. In *European Conference on Computer Vision*, 2020b.

Liang, J., Hu, D., and Feng, J. Domain adaptation with auxiliary target domain-oriented classifier. In *IEEE Conference on Computer Vision and Pattern Recognition*, 2021.

Liang, J., Hu, D., Feng, J., and He, R. Dine: Domain adaptation from single and multiple black-box predictors. In *IEEE Conference on Computer Vision and Pattern Recognition*, 2022.

Lipton, Z., Wang, Y.-X., and Smola, A. Detecting and correcting for label shift with black box predictors. In *International Conference on Machine Learning*, 2018.

Liu, B., Ben Ayed, I., Galdran, A., and Dolz, J. The devil is in the margin: Margin-based label smoothing for network calibration. In *IEEE Conference on Computer Vision and Pattern Recognition*, 2022.

Long, M., Cao, Y., Wang, J., and Jordan, M. Learning transferable features with deep adaptation networks. In *International Conference on Machine Learning*, 2015.

Long, M., Cao, Z., Wang, J., and Jordan, M. I. Conditional adversarial domain adaptation. In *Advances in Neural Information Processing Systems*, 2018.

Louizos, C. and Welling, M. Multiplicative normalizing flows for variational bayesian neural networks. In *International Conference on Machine Learning*, 2017.

Ovadia, Y., Fertig, E., Ren, J., Nado, Z., Sculley, D., Nowozin, S., Dillon, J., Lakshminarayanan, B., and Snoek, J. Can you trust your model's uncertainty? evaluating predictive uncertainty under dataset shift. In *Advances in Neural Information Processing Systems*, 2019.

Pan, S. J. and Yang, Q. A survey on transfer learning. *IEEE Transactions on Knowledge and Data Engineering*, 22 (10):1345–1359, 2009.

Panareda Busto, P. and Gall, J. Open set domain adaptation. In *IEEE International Conference on Computer Vision*, 2017.

Park, S., Bastani, O., Weimer, J., and Lee, I. Calibrated prediction with covariate shift via unsupervised domain adaptation. In *International Conference on Artificial Intelligence and Statistics*, 2020.

Peng, X., Usman, B., Kaushik, N., Hoffman, J., Wang, D., and Saenko, K. Visda: The visual domain adaptation challenge. *arXiv preprint arXiv:1710.06924*, 2017.

Peng, X., Bai, Q., Xia, X., Huang, Z., Saenko, K., and Wang, B. Moment matching for multi-source domain adaptation. In *IEEE International Conference on Computer Vision*, 2019.

Platt, J. et al. Probabilistic outputs for support vector machines and comparisons to regularized likelihood methods. *Advances in Large Margin Classifiers*, 10(3):61–74, 1999.

Richter, S. R., Vineet, V., Roth, S., and Koltun, V. Playing for data: Ground truth from computer games. In *European Conference on Computer Vision*, 2016.

Ros, G., Sellart, L., Materzynska, J., Vazquez, D., and Lopez, A. M. The synthia dataset: A large collection of synthetic images for semantic segmentation of urban scenes. In *IEEE Conference on Computer Vision and Pattern Recognition*, 2016.

Saenko, K., Kulis, B., Fritz, M., and Darrell, T. Adapting visual category models to new domains. In *European Conference on Computer Vision*, 2010.

Saito, K., Watanabe, K., Ushiku, Y., and Harada, T. Maximum classifier discrepancy for unsupervised domain adaptation. In *IEEE Conference on Computer Vision and Pattern Recognition*, 2018.

Saito, K., Kim, D., Sclaroff, S., Darrell, T., and Saenko, K. Semi-supervised domain adaptation via minimax entropy. In *IEEE International Conference on Computer Vision*, 2019.

Salvador, T., Voleti, V., Iannantuono, A., and Oberman, A. Improved predictive uncertainty using corruption-based calibration. *STAT*, 1050:7, 2021.

Shu, R., Bui, H. H., Narui, H., and Ermon, S. A dirt-t approach to unsupervised domain adaptation. *arXiv preprint arXiv:1802.08735*, 2018.

Sohn, K., Berthelot, D., Carlini, N., Zhang, Z., Zhang, H., Raffel, C. A., Cubuk, E. D., Kurakin, A., and Li, C.-L. Fixmatch: Simplifying semi-supervised learning with consistency and confidence. In *Advances in Neural Information Processing Systems*, 2020.

Sugiyama, M., Krauledat, M., and Müller, K.-R. Covariate shift adaptation by importance weighted cross validation. *Journal of Machine Learning Research*, 8(5), 2007.

Thulasidasan, S., Chennupati, G., Bilmes, J. A., Bhattacharya, T., and Michalak, S. On mixup training: Improved calibration and predictive uncertainty for deep neural networks. In *Advances in Neural Information Processing Systems*, 2019.

Tomani, C., Gruber, S., Erdem, M. E., Cremers, D., and Buettner, F. Post-hoc uncertainty calibration for domain drift scenarios. In *IEEE Conference on Computer Vision and Pattern Recognition*, 2021.

Tomani, C., Waseda, F. K., Shen, Y., and Cremers, D. Beyond in-domain scenarios: Robust density-aware calibration. In *International Conference on Machine Learning*, 2023.

Tsai, Y.-H., Hung, W.-C., Schulter, S., Sohn, K., Yang, M.-H., and Chandraker, M. Learning to adapt structured output space for semantic segmentation. In *IEEE Conference on Computer Vision and Pattern Recognition*, 2018.

Venkateswara, H., Eusebio, J., Chakraborty, S., and Panchanathan, S. Deep hashing network for unsupervised domain adaptation. In *IEEE Conference on Computer Vision and Pattern Recognition*, 2017.

Verma, V., Lamb, A., Beckham, C., Najafi, A., Mitliagkas, I., Lopez-Paz, D., and Bengio, Y. Manifold mixup: Better representations by interpolating hidden states. In *International Conference on Machine Learning*, 2019.

Verma, V., Kawaguchi, K., Lamb, A., Kannala, J., Solin, A., Bengio, Y., and Lopez-Paz, D. Interpolation consistency training for semi-supervised learning. *Neural Networks*, 145:90–106, 2022.

Wang, H., Ge, S., Lipton, Z., and Xing, E. P. Learning robust global representations by penalizing local predictive power. In *Advances in Neural Information Processing Systems*, 2019.

Wang, X., Long, M., Wang, J., and Jordan, M. Transferable calibration with lower bias and variance in domain adaptation. In *Advances in Neural Information Processing Systems*, 2020.

Wen, Y., Vicol, P., Ba, J., Tran, D., and Grosse, R. Flipout: Efficient pseudo-independent weight perturbations on mini-batches. *arXiv preprint arXiv:1803.04386*, 2018.

Xu, R., Li, G., Yang, J., and Lin, L. Larger norm more transferable: An adaptive feature norm approach for unsupervised domain adaptation. In *IEEE International Conference on Computer Vision*, 2019.

Yu, Y., Bates, S., Ma, Y., and Jordan, M. Robust calibration with multi-domain temperature scaling. In *Advances in Neural Information Processing Systems*, 2022.

Yun, S., Han, D., Oh, S. J., Chun, S., Choe, J., and Yoo, Y. Cutmix: Regularization strategy to train strong classifiers with localizable features. In *IEEE International Conference on Computer Vision*, 2019.

Zadrozny, B. and Elkan, C. Obtaining calibrated probability estimates from decision trees and naive bayesian classifiers. In *International Conference on Machine Learning*, 2001.

Zhang, H., Cisse, M., Dauphin, Y. N., and Lopez-Paz, D. mixup: Beyond empirical risk minimization. In *International Conference on Learning Representations*, 2018.

Zhang, H., Zhang, Y., Jia, K., and Zhang, L. Unsupervised domain adaptation of black-box source models. *arXiv preprint arXiv:2101.02839*, 2021.

Zou, Y., Deng, W., and Zheng, L. Adaptive calibrator ensemble: Navigating test set difficulty in out-of-distribution scenarios. In *IEEE International Conference on Computer Vision*, 2023.

A. Algorithm

The PyTorch-style pseudocode for our calibration method PseudoCal is provided in Algorithm 1.

B. Additional Calibration Metrics

In addition to the Expected Calibration Error (ECE) (Guo et al., 2017), we consider two extra calibration metrics as follows. Let $\mathbf{y}_i$ represent the one-hot ground truth encoding for input sample x_i, and $\hat{\mathbf{p}}_i$ denote the predicted probability vector output by the model ϕ.

Negative Log-Likelihood (NLL) (Goodfellow et al., 2016) is also known as the cross-entropy loss. The NLL loss for a single sample x_i is given by:

$$\mathcal{L}_{\text{NLL}} = -\sum_{c=1}^{C} \mathbf{y}_i^c \log \hat{\mathbf{p}}_i^c$$

Brier Score (BS) (Brier et al., 1950) can be defined as the squared error between the predicted probability vector and the one-hot label vector. The Brier Score for a single sample x_i is given by:

$$\mathcal{L}_{\text{BS}} = \frac{1}{C}\sum_{c=1}^{C} (\hat{\mathbf{p}}_i^c - \mathbf{y}_i^c)^2$$

Similar to the ViT results presented in Table 9, we have observed consistent advantages of our PseudoCal method over existing calibration methods across all three calibration metrics: ECE, NLL, and BS. We choose to report the ECE results for most of the experiments because ECE (Guo et al., 2017) is a widely used calibration metric.

C. Semantic Segmentation Calibration Details

For our calibration experiments on semantic segmentation, we calibrate the models trained solely on the source domain (GTA5 (Richter et al., 2016) or SYNTHIA (Ros et al., 2016)) without any target domain adaptation. We treat each pixel as an individual sample in classification tasks for both *mixup* and *temperature scaling*. To address the computational complexity, we adopt the evaluation strategy suggested in previous studies (de Jorge et al., 2023) and randomly sample 20,000 pixels from each image (with resolutions such as 1920*720) for calibration.

D. Analysis of Sample-Level Correspondence

In the **Analysis** part of Section 3.2 in the main text, we offer an intuitive analysis of the sample-level correspondence between pseudo-target data and real target samples. Figure 1(b) qualitatively illustrates the striking similarity in the correct-wrong statistics between the real target and pseudo target. To further enhance the understanding of this correspondence, we aim for a quantitative sample-level analysis. Consider a pair of real samples x_{t}^i with pseudo-label $\hat{y}_{\text{t}}^i$ inferred by the UDA model ϕ, and x_{t}^j with pseudo-label $\hat{y}_{\text{t}}^j$. We employ the *mixup* operation to generate a mixed sample x_{pt}^i with the mixed label y_{pt}^i. For simplicity, we assume that all labels are one-hot hard labels and λ is in the range of $(0.5, 1.0)$. This implies that x_{t}^i functions as the primary real sample, directly determining the mixed label y_{pt}^i, i.e., $y_{\text{pt}}^i == \hat{y}_{\text{t}}^i$. We apply the *mixup* operation n_{t} times during the model inference stage using unlabeled target data. This results in a labeled pseudo-target set $\{(x_{\text{pt}}^i, y_{\text{pt}}^i)\}_{i=1}^{n_{\text{t}}}$ and the original pseudo-labeled real target set $\{(x_{\text{t}}^i, \hat{y}_{\text{t}}^i)\}_{i=1}^{n_{\text{t}}}$. Using the same UDA model ϕ, we infer predictions $\hat{y}_{\text{pt}}^i$ for the mixed sample x_{pt}^i and traverse through all mixed samples. For the mixed pseudo-target samples, we obtain predictions $\{\hat{y}_{\text{pt}}^i\}_{i=1}^{n_{\text{t}}}$ and corresponding labels $\{y_{\text{pt}}^i\}_{i=1}^{n_{\text{t}}}$. Regarding real target samples, the predictions are the available pseudo-labels $\{\hat{y}_{\text{t}}^i\}_{i=1}^{n_{\text{t}}}$, while the labels are ground truth labels $\{y_{\text{t}}^i\}_{i=1}^{n_{\text{t}}}$ which are used to assess the UDA model accuracy.

$$\text{CR}_{\text{correct}} = \frac{\sum_i^{n_{\text{t}}} (\hat{y}_{\text{pt}}^i == y_{\text{pt}}^i) \cdot (\hat{y}_{\text{t}}^i == y_{\text{t}}^i)}{\sum_i^{n_{\text{t}}} (\hat{y}_{\text{t}}^i == y_{\text{t}}^i)}$$

$$\text{CR}_{\text{wrong}} = \frac{\sum_i^{n_{\text{t}}} (\hat{y}_{\text{pt}}^i \neq y_{\text{pt}}^i) \cdot (\hat{y}_{\text{t}}^i \neq y_{\text{t}}^i)}{\sum_i^{n_{\text{t}}} (\hat{y}_{\text{t}}^i \neq y_{\text{t}}^i)}$$

$$\text{CR}_{\text{arithmetic}} = \frac{1}{n_{\text{t}}} \cdot \left[\sum_i^{n_{\text{t}}} (\hat{y}_{\text{pt}}^i == y_{\text{pt}}^i) \cdot (\hat{y}_{\text{t}}^i == y_{\text{t}}^i) + \sum_i^{n_{\text{t}}} (\hat{y}_{\text{pt}}^i \neq y_{\text{pt}}^i) \cdot (\hat{y}_{\text{t}}^i \neq y_{\text{t}}^i) \right]$$

$$\text{CR}_{\text{harmonic}} = \frac{2 \cdot \text{CR}_{\text{correct}} \cdot \text{CR}_{\text{wrong}}}{\text{CR}_{\text{correct}} + \text{CR}_{\text{wrong}}}$$

Using these predictions and labels, we can systematically quantify the sample-level correspondence between the pseudo and real target sets for a more in-depth understanding. We establish such correspondence when both the predictions of a mixed pseudo sample and its primary real sample are either both correct or both wrong, as assessed by their respective labels. In other words, we consider a correspondence when $\hat{y}_{\text{pt}}^i == y_{\text{pt}}^i$ and $\hat{y}_{\text{t}}^i == y_{\text{t}}^i$, or when $\hat{y}_{\text{pt}}^i \neq y_{\text{pt}}^i$ and $\hat{y}_{\text{t}}^i \neq y_{\text{t}}^i$. To quantitatively measure this sample-level correspondence, we introduce four correspondence metrics. The first metric, denoted as $\text{CR}_{\text{correct}}$, represents the correspondence rate of correct real samples. It indicates how many correct real samples maintain correspondence with their mixed counterparts. Similarly, our second metric, denoted as CR_{wrong}, measures the correspondence

Algorithm 1 PyTorch-style pseudocode for PseudoCal.

```
# x: A batch of real target images with shuffled order.
# lam: The mix ratio, a fixed scalar value between 0.5 and 1.0.
# net: A trained UDA model in the evaluation mode.

# Perform pseudo-target synthesis for a mini-batch.
def pseudo_target_synthesis(x, lam, net):

    # Use the random index within the data batch
    # to obtain a pair of real samples for mixup.
    rand_idx = torch.randperm(x.shape[0])
    inputs_a = x
    inputs_b = x[rand_idx]

    # Obtain model predictions and pseudo labels (pl).
    pred_a = net(inputs_a)
    pl_a = pred_a.max(dim=1)[1]
    pl_b = pl_a[rand_idx]

    # Select the samples with distinct labels for the mixup.
    diff_idx = (pl_a != pl_b).nonzero(as_tuple=True)[0]

    # Mixup with images and labels.
    pseudo_target_x = lam * inputs_a + (1 - lam) * inputs_b

    # If the user is not aware that lam is between 0.5 and 1.0,
    # the following if-else code can avoid bugs.
    if lam > 0.5:
        pseudo_target_y = pl_a
    else:
        pseudo_target_y = pl_b

    return pseudo_target_x[diff_idx], pseudo_target_y[diff_idx]

# Perform supervised calibration using pseudo-target data.
def pseudoCal(x, lam, net):

    # Synthesize a mini-batch of pseudo-target samples and labels.
    pseudo_x, pseudo_y = pseudo_target_synthesis(x, lam, net)

    # Infer the logits for the pseudo-target samples.
    pseudo_logit = net(pseudo_x)

    # Apply temperature scaling to estimate the
    # pseudo-target temperature as the real temperature.
    calib_method = TempScaling()
    pseudo_temp = calib_method(pseudo_logit, pseudo_y)

    return pseudo_temp
```

rate of wrong real samples. For a more comprehensive perspective, we introduce the third metric, $\mathrm{CR}_{\mathrm{arithmetic}}$, which calculates the arithmetic mean of $\mathrm{CR}_{\mathrm{correct}}$ and $\mathrm{CR}_{\mathrm{wrong}}$, assessing the correspondence rate of all real samples. However, it's important to note that these three metrics may be misleading in extreme situations where most of the correspondences are biased toward either being correct or wrong. To address this issue, we propose our fourth metric, $\mathrm{CR}_{\mathrm{harmonic}}$, which takes the harmonic mean of $\mathrm{CR}_{\mathrm{correct}}$ and $\mathrm{CR}_{\mathrm{wrong}}$, providing equal consideration to both correct and wrong correspondences. This metric is inspired by the success of the H-Score solution (Fu et al., 2020; Bucci et al., 2020) in balanced accuracy measurement for known-unknown accuracy in open-set UDA.

For empirical illustration, we conduct experiments using PseudoCal with varied λ values of $\{0.51, 0.65, 1.0\}$, among which 0.65 is our default value for all experiments in the main text. We report all results, including the measurement results of the sample-level correspondence using the four metrics described above, in Table 11. From these results, we have three consistent observations: *i)* As expected, only the harmonic metric $\mathrm{CR}_{\mathrm{harmonic}}$ is reliable and aligns with

Table 11: By tuning the mix ratio λ, we can synthesize the most ambiguous pseudo samples ($\lambda = 0.51$) and the simplest ones ($\lambda = 1.0$), i.e., the pseudo-labeled real samples themselves. PseudoCal employs a moderate value of $\lambda = 0.65$ for all the results. Under these three cases, we measure the sample-level correspondence between the real samples and pseudo samples using four correspondence metrics.

Method	MCD		BNM		CDAN	SHOT	PADA		DINE
	D→A	W→A	Cl→Pr	Pr→Re	R→C	I→S	Ar→Cl	Re→Ar	P→R
No Calib. ECE (%)	16.39	17.03	22.09	15.72	9.83	34.71	20.35	8.31	12.39
PseudoCal (λ=1.0)	32.47	33.35	26.31	19.65	47.02	65.70	56.18	36.27	19.31
PseudoCal (λ=0.65)	**4.38**	**4.06**	**6.31**	**4.76**	**1.51**	**8.42**	**2.95**	**3.71**	**5.29**
PseudoCal (λ=0.51)	13.77	11.69	11.85	14.13	15.15	11.08	11.03	23.07	14.50
Oracle ECE (%)	2.31	1.90	3.14	1.10	1.28	4.39	2.16	2.87	1.29
Accuracy (%)	67.52	66.63	73.69	80.35	52.98	34.29	43.82	63.73	80.69
# of correct real data	1826	1792	3183	3408	9650	17218	703	656	55757
# of wrong real data	872	894	1135	836	8548	32998	918	385	13342
$\text{CR}_{\text{harmonic}}$ (λ=1.0) (%)	0	0	0	0	0	0	0	0	0
$\text{CR}_{\text{harmonic}}$ (λ=0.65) (%)	**63.45**	**63.45**	**59.89**	**59.27**	**60.56**	**56.28**	**60.21**	**62.04**	**61.73**
$\text{CR}_{\text{harmonic}}$ (λ=0.51) (%)	52.08	54.42	53.13	52.87	45.33	35.18	50.94	46.03	56.26
$\text{CR}_{\text{arithmetic}}$ (λ=1.0) (%)	**67.68**	**66.72**	**73.71**	**80.30**	53.03	34.29	43.37	**63.02**	**80.69**
$\text{CR}_{\text{arithmetic}}$ (λ=0.65) (%)	62.36	62.75	61.72	63.08	**61.58**	65.58	**63.92**	61.00	70.73
$\text{CR}_{\text{arithmetic}}$ (λ=0.51) (%)	52.07	54.10	50.03	47.51	56.35	**66.48**	63.02	50.52	50.74
$\text{CR}_{\text{correct}}$ (λ=1.0) (%)	**100**	**100**	**100**	**100**	**100**	**100**	**100**	**100**	**100**
$\text{CR}_{\text{correct}}$ (λ=0.65) (%)	59.93	61.16	63.52	65.22	52.09	44.48	50.74	56.02	75.11
$\text{CR}_{\text{correct}}$ (λ=0.51) (%)	38.53	41.35	41.69	40.54	30.90	21.88	36.67	31.94	44.76
CR_{wrong} (λ=1.0) (%)	0	0	0	0	0	0	0	0	0
CR_{wrong} (λ=0.65) (%)	67.40	65.92	56.66	54.32	72.31	76.60	74.04	69.52	52.40
CR_{wrong} (λ=0.51) (%)	**80.32**	**79.57**	**73.2**	**75.99**	**85.04**	**89.75**	**83.38**	**82.39**	**75.73**

the actual calibration performance, while both the one-sided correct measure $\text{CR}_{\text{correct}}$ and the wrong measure CR_{wrong} can be extremely biased, which would further directly mislead the arithmetic mean metric $\text{CR}_{\text{arithmetic}}$. *2)* Similar to the discussion on the impact of mix ratio (λ) in Section 4.3, our observations reveal that λ values near 0.5 predominantly yield wrong predictions for pseudo-target samples (mixed samples), while λ values of 1.0 result in entirely correct predictions. The role of λ in controlling cross-cluster perturbation, determining the difficulty of mixed samples, is noteworthy. A λ close to 0.5 generates ambiguous mixed samples with almost even contributions from two real samples bearing different pseudo-labels. In such instances, the UDA model struggles to ascertain the class label, resulting in predominantly wrong predictions when evaluated with mixed labels. Conversely, a λ of 1.0 equates to not using *mixup* and directly leveraging pseudo-labeled real target samples. This scenario constitutes the easiest mixed samples, as the UDA model outputs predictions identical to raw target predictions, leading to entirely correct predictions when assessed with target pseudo-labels. From the *cluster assumption* perspective, extreme λ values render the relevant analysis inconclusive. A λ value very close to 0.5 makes it challenging to determine the primary real sample. Conversely, a λ value very close to 1.0 signifies the negligible cross-cluster perturbation, generating a mixed sample nearly identical to the primary real sample, wherein the cluster assumption does not apply. In general, extreme λ values, whether close to 0.5 or 1.0, exhibit significant bias towards either wrong or correct predictions, which indicates correct-wrong statistics of the pseudo-target set become skewed, deviating from real target samples. Hence, for a typical UDA model with both correct and wrong target predictions, we recommend employing a moderate λ value, such as the 0.65 utilized in our main text. *(iii)* Taking a closer look at the reliable measure of sample-level correspondence by $\text{CR}_{\text{harmonic}}$, we find that for various UDA models, there maintains a high correspondence with a $\text{CR}_{\text{harmonic}}$ value of about 60%, even for a low-accuracy model with only 30% accuracy. This strongly supports the robust existence of the *cluster assumption* and the robustness of our analysis in Section 3.2. For a vivid illustration of the impact of λ values on sample-level correspondence, Figure 4 presents the correct-wrong statistics of all UDA methods outlined in Table 11. We find that extreme λ values result in a notable skewness in the correct-wrong statistics of the pseudo-target set when compared to the real target set. For a clear visualization of mixed images, please see Figure 5.

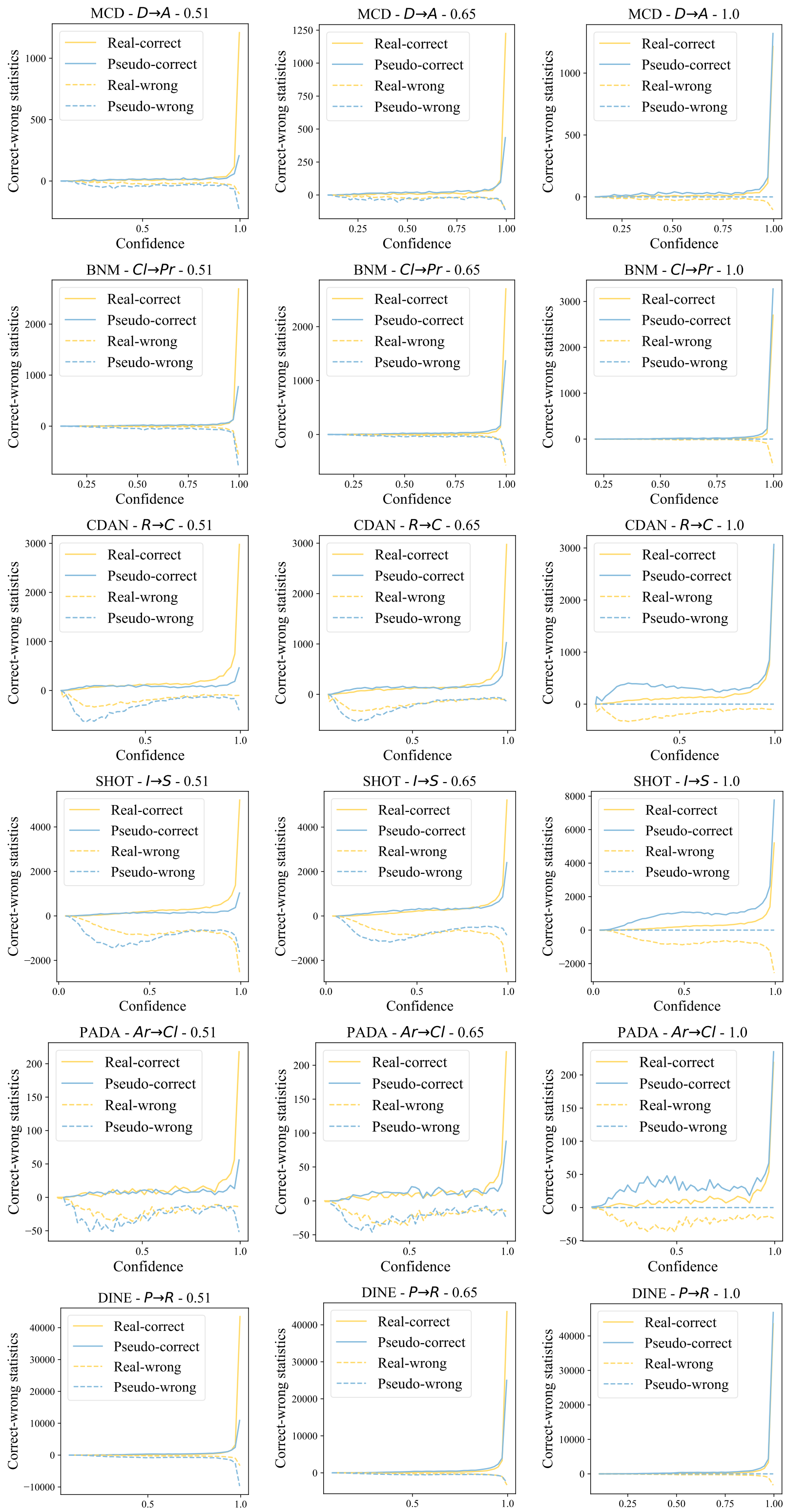

(a) $\lambda = 0.51$ (b) $\lambda = 0.65$ (c) $\lambda = 1.0$

Figure 4: The correct-wrong statistics are computed for both the pseudo-target and real target sets. We partition confidence values into 50 bins and present the count of correct and wrong predictions in each bin. Correctness for real target data is determined by comparing predictions of real target samples with ground truths. For pseudo-target data, correctness is assessed by comparing predictions of the mixed samples with mixed labels.

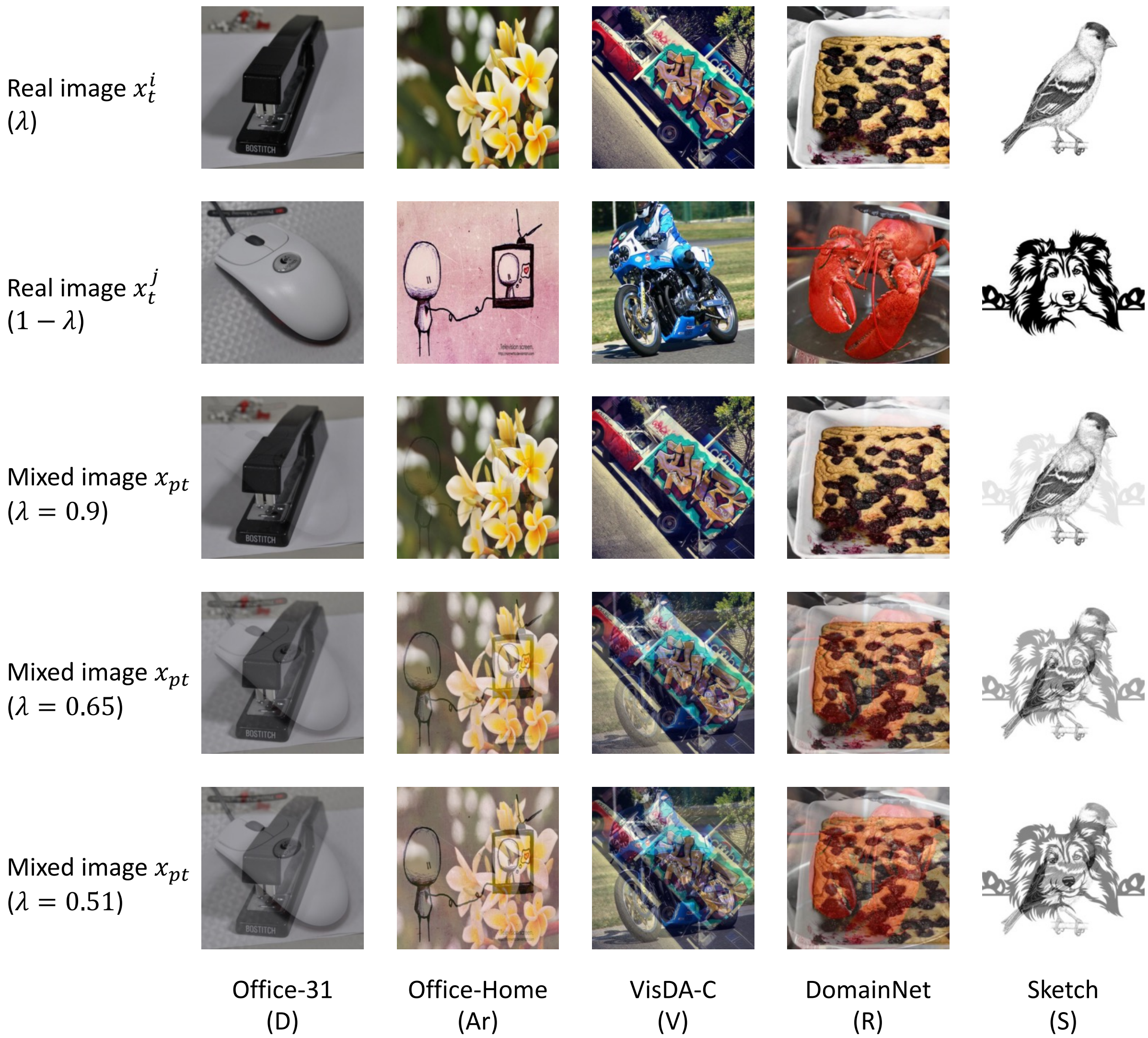

Figure 5: Visualization of input-level *mixup* for various UDA benchmarks with varied λ values.

Table 12: ECE (%) of calibration results when combining PseudoCal with different supervised calibration methods, including MatrixScal (Guo et al., 2017), VectorScal (Guo et al., 2017), and TempScal (Guo et al., 2017) (our default choice).

Method	MCD		BNM		CDAN	SHOT	PADA		DINE
	D→A	W→A	Cl→Pr	Pr→Re	R→C	I→S	Ar→Cl	Re→Ar	P→R
No Calib.	16.39	17.03	22.09	15.72	9.83	34.71	20.35	8.31	12.39
MatrixScal-src	17.86	20.28	25.73	15.98	22.11	-	36.55	20.45	-
VectorScal-src	17.75	20.52	16.40	12.36	12.88	-	20.53	9.07	-
TempScal-src	32.09	18.65	15.10	11.64	9.27	-	15.15	6.34	-
PseudoCal(Matrix.)	11.61	13.20	16.07	11.83	15.09	42.86	35.85	27.07	7.65
PseudoCal(Vector.)	11.00	9.32	9.31	6.05	6.37	23.90	5.90	4.19	6.23
PseudoCal(Temp.)	**4.38**	**4.06**	**6.31**	**4.76**	**1.51**	**8.42**	**2.95**	**3.71**	**5.29**
Oracle	2.31	1.90	3.14	1.10	1.28	4.39	2.16	2.87	1.29
Accuracy (%)	67.52	66.63	73.69	80.35	52.98	34.29	43.82	63.73	80.69

E. Full Calibration Results

Due to space constraints in the main text, we have presented the averaged results for tasks with the same target domain. For example, in the case of *Office-Home*, UDA tasks including 'Cl→Ar', 'Pr→Ar', and 'Re→Ar' share the common target domain 'Ar'. Consequently, we have averaged the results of these three UDA tasks and reported the averaged value in the tables within our main text under the column labeled '→ Ar'. Additionally, note that the 'avg' column represents the averaged results within each UDA method's columns to the left of the 'avg' column. Differently, the 'AVG' column signifies the averaged results across all 'avg' columns associated with different UDA methods. Consequently, the 'AVG' column can be considered more reliable and representative for drawing conclusions.

Additionally, as *matrix scaling* (MatrixScal), *vector scaling* (VectorScal), and *temperature scaling* (TempScal) are similar, all proposed by (Guo et al., 2017), and the authors have demonstrated that *temperature scaling* (TempScal) is the superior solution. Therefore, as for the source-domain calibration baseline (using a labeled source validation set for calibration), we have only reported the results of TempScal-src in the tables in the main text. Here, we present the results of MatrixScal-src and VectorScal-src for additional reference, without impacting any of the conclusions drawn in the main text. While our PseudoCal is inspired by the factorized NLL of TempScal and naturally employs TempScal as the default supervised calibration method for our synthesized labeled pseudo-target set, we investigate the compatibility of PseudoCal with alternative supervised calibration methods, such as MatrixScal and VectorScal. The corresponding results are detailed in Table 12. Our findings reveal two key observations: *1)* If a supervised calibration method exhibits stability and effectiveness with the source labeled data, combining it with PseudoCal tends to yield reduced ECE error compared to the no calibration baseline. *2)* Due to the similarity in correct-wrong statistics between the pseudo-target set and real target data, PseudoCal demonstrates compatibility with both MatrixScal and VectorScal. However, it consistently achieves the best calibration performance when paired with TempScal, aligning with the conclusion in (Guo et al., 2017) that TempScal generally outperforms MatrixScal and VectorScal. For detailed calibration results for each task, please refer to Table 13 through Table 31.

Table 13: ECE (%) of a closed-set UDA method ATDOC (Liang et al., 2021) on *Office-Home*.

Method	Ar $\to$ Cl	Ar $\to$ Pr	Ar $\to$ Re	Cl $\to$ Ar	Cl $\to$ Pr	Cl $\to$ Re	Pr $\to$ Ar	Pr $\to$ Cl	Pr $\to$ Re	Re $\to$ Ar	Re $\to$ Cl	Re $\to$ Pr	avg
No Calib.	22.83	10.57	6.31	10.77	8.88	6.38	10.39	22.61	5.49	9.06	21.61	6.38	11.77
MatrixScal-src	35.03	20.72	18.28	27.54	24.73	23.40	22.51	32.85	13.66	20.25	32.89	12.90	23.73
VectorScal-src	22.05	10.09	5.85	11.51	7.74	6.01	15.12	26.85	7.81	7.94	21.10	5.03	12.26
TempScal-src	14.69	5.55	**2.60**	4.27	**3.17**	**1.45**	9.67	22.55	5.04	4.63	15.37	**3.21**	7.68
CPCS	8.37	9.32	6.44	12.94	14.94	11.41	12.28	6.00	4.13	17.18	29.88	8.80	11.81
TransCal	4.95	13.85	16.58	17.29	17.34	18.76	18.77	7.48	19.54	18.20	7.13	16.90	14.73
Ensemble	18.40	7.47	4.51	7.82	4.76	4.24	8.36	17.96	**3.92**	5.96	17.68	4.29	8.78
PseudoCal (ours)	**3.07**	**4.23**	5.28	**1.96**	6.27	5.70	**2.52**	**4.05**	4.22	**2.79**	**1.68**	7.03	**4.07**
Oracle	2.38	3.14	2.34	1.44	1.92	1.36	1.98	1.92	1.37	1.71	1.43	1.80	1.90
Accuracy (%)	52.07	74.48	79.27	64.24	73.85	75.42	64.65	50.65	78.54	70.37	54.46	81.48	68.29

Table 14: ECE (%) of a closed-set UDA method BNM (Cui et al., 2020) on *Office-Home*.

Method	Ar $\to$ Cl	Ar $\to$ Pr	Ar $\to$ Re	Cl $\to$ Ar	Cl $\to$ Pr	Cl $\to$ Re	Pr $\to$ Ar	Pr $\to$ Cl	Pr $\to$ Re	Re $\to$ Ar	Re $\to$ Cl	Re $\to$ Pr	avg
No Calib.	38.64	22.49	16.21	30.89	22.09	18.25	34.90	42.46	15.72	27.11	38.44	14.52	26.81
MatrixScal-src	39.37	23.31	19.01	30.30	25.73	22.24	31.37	41.37	15.98	24.06	37.39	14.77	27.07
VectorScal-src	30.83	17.66	9.97	21.91	16.40	11.46	27.76	37.27	12.36	18.91	29.06	10.03	20.30
TempScal-src	27.22	16.34	8.91	20.39	15.10	10.21	28.82	35.60	11.64	20.12	28.15	9.67	19.35
CPCS	33.80	18.08	8.12	17.24	19.77	7.90	28.68	**17.28**	10.39	28.36	23.97	6.86	18.37
TransCal	25.75	12.11	5.87	15.73	10.51	5.51	21.41	29.66	5.02	**15.17**	26.25	4.80	14.82
Ensemble	29.52	16.03	12.00	22.77	15.55	14.06	25.17	32.06	11.53	19.55	30.46	11.56	20.02
PseudoCal (ours)	**14.27**	**8.74**	**4.60**	**15.46**	**6.31**	**4.69**	**20.90**	18.35	**4.76**	15.66	**15.47**	**3.55**	**11.06**
Oracle	3.16	2.18	1.76	2.00	3.14	1.95	2.92	1.78	1.10	1.68	2.64	1.77	2.17
Accuracy (%)	54.39	73.49	79.78	64.52	73.69	76.82	61.68	51.13	80.35	70.05	55.56	82.36	68.65

Table 15: ECE (%) of a closed-set UDA method MCC (Jin et al., 2020) on *Office-Home*.

Method	Ar $\to$ Cl	Ar $\to$ Pr	Ar $\to$ Re	Cl $\to$ Ar	Cl $\to$ Pr	Cl $\to$ Re	Pr $\to$ Ar	Pr $\to$ Cl	Pr $\to$ Re	Re $\to$ Ar	Re $\to$ Cl	Re $\to$ Pr	avg
No Calib.	23.74	14.31	10.89	12.70	13.15	11.72	14.36	23.18	8.98	12.69	22.40	9.54	14.81
MatrixScal-src	37.39	23.28	19.95	31.00	27.75	25.27	26.13	35.70	16.27	21.56	35.20	14.95	26.20
VectorScal-src	21.05	12.79	7.87	10.96	11.18	8.20	16.87	28.29	9.64	7.58	21.40	6.15	13.50
TempScal-src	12.23	6.43	3.61	4.06	4.69	**2.85**	11.38	22.91	5.83	4.79	13.60	**4.11**	8.04
CPCS	25.11	15.31	**3.60**	19.41	14.36	4.49	13.83	35.66	8.56	24.08	24.99	14.27	16.97
TransCal	3.04	6.31	5.98	12.75	7.42	8.60	11.95	4.59	9.90	10.48	3.95	6.37	7.61
Ensemble	19.20	11.30	8.05	10.01	9.69	8.51	10.11	18.98	7.13	9.15	19.42	7.44	11.58
PseudoCal (ours)	**2.71**	**5.04**	3.81	**3.17**	**4.64**	3.06	**2.66**	**1.54**	**3.85**	**2.73**	**2.51**	5.86	**3.47**
Oracle	2.41	2.57	2.31	2.67	1.73	1.62	1.58	0.84	1.80	2.51	1.66	2.35	2.00
Accuracy (%)	47.26	69.29	75.90	59.91	68.33	70.16	56.32	44.49	76.04	66.87	50.65	79.48	63.73

Table 16: ECE (%) of a closed-set UDA method CDAN (Long et al., 2018) on *Office-Home*.

Method	Ar $\to$ Cl	Ar $\to$ Pr	Ar $\to$ Re	Cl $\to$ Ar	Cl $\to$ Pr	Cl $\to$ Re	Pr $\to$ Ar	Pr $\to$ Cl	Pr $\to$ Re	Re $\to$ Ar	Re $\to$ Cl	Re $\to$ Pr	avg
No Calib.	24.88	14.66	10.39	14.71	13.05	11.25	13.24	22.54	8.37	12.19	21.41	8.74	14.62
MatrixScal-src	35.03	22.64	19.14	28.14	26.14	22.96	24.20	33.34	15.03	20.32	30.69	13.78	24.28
VectorScal-src	18.81	10.46	7.24	8.92	9.81	6.73	15.31	26.51	9.18	7.51	16.70	5.76	11.91
TempScal-src	12.48	5.82	3.40	**5.57**	5.14	3.06	9.78	21.29	6.12	5.31	12.55	**4.06**	7.88
CPCS	31.45	13.21	2.36	25.84	24.68	17.24	13.44	27.86	10.09	15.85	41.38	7.98	19.28
TransCal	**2.65**	11.04	11.67	14.44	13.41	14.01	16.34	6.04	15.50	13.51	5.46	11.77	11.32
Ensemble	18.64	11.85	7.23	10.87	9.04	7.94	9.45	19.12	6.52	9.90	17.97	6.56	11.26
PseudoCal (ours)	3.52	**4.33**	**2.32**	5.67	**4.81**	**2.82**	**6.36**	**3.78**	**2.05**	**3.28**	**3.85**	5.00	**3.98**
Oracle	1.83	2.96	1.94	3.88	1.74	2.20	4.46	3.22	1.68	2.50	3.48	2.08	2.66
Accuracy (%)	48.00	67.00	75.07	59.83	66.88	69.98	58.59	48.64	76.31	68.36	53.33	79.68	64.31

Table 17: ECE (%) of a closed-set UDA method SAFN (Xu et al., 2019) on *Office-Home*.

Method	Ar $\to$ Cl	Ar $\to$ Pr	Ar $\to$ Re	Cl $\to$ Ar	Cl $\to$ Pr	Cl $\to$ Re	Pr $\to$ Ar	Pr $\to$ Cl	Pr $\to$ Re	Re $\to$ Ar	Re $\to$ Cl	Re $\to$ Pr	avg
No Calib.	28.25	15.29	12.40	16.62	14.10	12.45	18.17	29.68	10.94	14.92	25.77	10.08	17.39
MatrixScal-src	37.63	23.66	20.05	28.07	26.01	23.00	25.60	37.84	16.22	20.98	33.18	14.69	25.58
VectorScal-src	21.01	12.78	9.20	10.96	10.28	7.67	16.03	26.93	8.91	10.72	20.21	6.35	13.42
TempScal-src	12.33	5.56	3.17	4.62	4.22	**3.40**	9.99	21.72	5.64	6.36	14.33	3.89	7.94
CPCS	31.45	16.18	10.90	23.93	11.19	6.71	15.78	25.66	18.73	5.24	34.50	**2.80**	16.92
TransCal	7.50	**4.23**	**2.80**	4.11	**3.63**	4.89	3.14	7.47	4.76	3.26	5.65	3.46	4.57
Ensemble	25.00	13.33	9.91	15.20	11.62	10.14	16.12	26.14	9.54	13.15	23.56	8.55	15.19
PseudoCal (ours)	**3.30**	6.41	4.14	**3.46**	7.06	5.18	**2.99**	**3.40**	**3.79**	**2.70**	**3.33**	7.12	**4.41**
Oracle	3.10	3.78	1.94	2.06	1.85	2.18	2.65	1.66	1.11	1.16	2.68	1.92	2.17
Accuracy (%)	50.65	70.96	75.81	64.44	70.42	72.30	62.55	49.55	77.16	70.54	55.51	79.97	66.66

Table 18: ECE (%) of a closed-set UDA method MCD (Saito et al., 2018) on *Office-Home*.

Method	Ar → Cl	Ar → Pr	Ar → Re	Cl → Ar	Cl → Pr	Cl → Re	Pr → Ar	Pr → Cl	Pr → Re	Re → Ar	Re → Cl	Re → Pr	avg
No Calib.	26.24	16.26	12.30	16.42	14.19	13.27	19.02	27.38	10.35	13.63	24.25	9.43	16.89
MatrixScal-src	41.44	28.57	22.89	34.21	27.91	26.19	28.46	39.91	18.20	22.91	36.82	16.58	28.67
VectorScal-src	21.79	12.62	8.36	11.89	7.19	7.75	17.75	27.43	8.99	10.10	20.83	5.72	13.37
TempScal-src	8.59	**4.59**	**2.87**	3.65	**2.79**	**2.90**	10.42	17.99	4.85	3.96	9.86	**3.29**	6.31
CPCS	20.66	11.43	21.72	27.95	11.22	11.03	24.03	12.63	10.13	23.42	48.48	7.86	19.21
TransCal	**2.43**	8.94	9.45	10.78	10.81	10.80	9.86	**2.07**	13.56	11.69	3.49	11.19	8.76
Ensemble	20.49	10.59	7.24	11.59	9.53	9.16	15.53	22.66	6.52	9.95	19.45	6.66	12.45
PseudoCal (ours)	2.52	4.93	3.93	**3.39**	6.57	3.70	**5.05**	2.68	**3.52**	**3.76**	**3.39**	7.28	**4.23**
Oracle	2.22	2.48	2.08	2.68	2.31	2.13	3.02	1.97	2.44	2.26	2.61	2.11	2.36
Accuracy (%)	46.55	63.75	73.01	57.44	64.86	67.45	53.81	42.77	73.72	65.88	51.07	77.63	61.49

Table 19: ECE (%) of a closed-set UDA method ATDOC (Liang et al., 2021) on *DomainNet*.

Method	C → S	P → C	P → R	R → C	R → P	R → S	S → P	avg
No Calib.	12.22	9.27	3.75	9.81	6.85	12.36	7.92	8.88
MatrixScal-src	34.30	27.58	15.58	23.23	18.37	28.05	27.44	24.94
VectorScal-src	16.19	11.45	3.97	15.11	10.19	19.26	9.52	12.24
TempScal-src	10.32	6.52	1.94	10.86	8.51	13.31	6.92	8.34
CPCS	12.87	13.31	4.46	8.25	5.11	13.90	4.34	8.89
TransCal	19.89	23.51	26.65	22.52	24.93	19.46	24.59	23.08
Ensemble	8.71	5.73	**1.59**	6.91	4.41	9.38	4.66	5.91
PseudoCal (ours)	**1.68**	**1.98**	2.51	**1.66**	**1.21**	**1.71**	**1.61**	**1.77**
Oracle	0.98	1.92	0.86	1.18	0.70	1.16	1.17	1.14
Accuracy (%)	53.74	56.51	74.95	55.59	61.65	50.41	59.64	58.93

Table 20: ECE (%) of a closed-set UDA method BNM (Cui et al., 2020) on *DomainNet*.

Method	C → S	P → C	P → R	R → C	R → P	R → S	S → P	avg
No Calib.	30.88	29.27	15.37	27.87	21.79	31.65	22.41	25.61
MatrixScal-src	37.91	31.17	18.31	26.82	22.33	32.31	28.64	28.21
VectorScal-src	23.10	20.02	9.88	21.80	14.83	26.68	14.18	18.64
TempScal-src	19.11	18.79	9.40	19.28	14.42	21.49	12.81	16.47
CPCS	14.45	13.75	7.98	**2.72**	4.35	**4.14**	11.50	8.41
TransCal	9.21	**6.31**	**5.82**	6.73	**1.69**	9.56	**1.98**	**5.90**
Ensemble	25.08	23.46	12.61	23.42	18.52	27.34	18.70	21.30
PseudoCal (ours)	**5.08**	12.43	6.18	8.10	5.20	6.64	6.82	7.21
Oracle	1.60	3.17	3.40	1.63	1.50	1.00	1.81	2.02
Accuracy (%)	52.90	55.52	74.30	57.71	63.95	51.61	62.30	59.76

Table 21: ECE (%) of a closed-set UDA method MCC (Jin et al., 2020) on *DomainNet*.

Method	C → S	P → C	P → R	R → C	R → P	R → S	S → P	avg
No Calib.	15.19	8.29	4.79	8.98	6.91	12.04	8.63	9.26
MatrixScal-src	36.95	28.60	15.99	23.92	18.95	29.54	28.72	26.10
VectorScal-src	18.52	11.63	4.49	15.98	10.72	20.86	10.71	13.27
TempScal-src	13.49	5.92	**2.36**	10.83	8.96	14.27	7.67	9.07
CPCS	29.26	15.02	3.44	3.03	6.00	5.15	2.66	9.22
TransCal	16.89	22.54	23.45	22.00	24.68	19.17	23.44	21.74
Ensemble	11.36	5.38	2.57	6.03	4.40	9.32	5.80	6.41
PseudoCal (ours)	**2.72**	**1.45**	2.38	**1.25**	**1.64**	**3.48**	**2.13**	**2.15**
Oracle	0.80	1.36	1.09	0.96	1.18	0.97	1.70	1.15
Accuracy (%)	47.65	51.27	71.62	50.51	59.02	45.14	56.46	54.52

Table 22: ECE (%) of a closed-set UDA method CDAN (Long et al., 2018) on *DomainNet*.

Method	C → S	P → C	P → R	R → C	R → P	R → S	S → P	avg
No Calib.	17.00	10.51	5.56	9.83	8.26	11.88	11.03	10.58
MatrixScal-src	35.28	27.82	15.80	22.11	18.34	27.24	27.76	24.91
VectorScal-src	17.44	10.88	4.37	12.88	9.45	17.90	9.81	11.82
TempScal-src	13.39	6.58	2.75	9.27	8.30	11.22	8.32	8.55
CPCS	**2.40**	17.27	5.57	4.24	6.75	11.42	**1.81**	7.07
TransCal	14.85	20.65	22.93	21.19	22.27	19.01	20.55	20.21
Ensemble	12.96	7.47	3.54	6.96	5.73	9.62	7.75	7.72
PseudoCal (ours)	3.48	**1.65**	**1.86**	**1.51**	**1.70**	**1.85**	2.08	**2.02**
Oracle	1.03	1.61	1.07	1.28	0.73	0.84	1.43	1.14
Accuracy (%)	49.07	53.25	71.82	52.98	60.75	49.11	57.51	56.36

Table 23: ECE (%) of a closed-set UDA method SAFN (Xu et al., 2019) on *DomainNet*.

Method	C → S	P → C	P → R	R → C	R → P	R → S	S → P	avg
No Calib.	21.82	17.98	10.15	17.90	13.63	20.70	15.25	16.78
MatrixScal-src	33.45	22.54	11.16	21.05	15.53	26.33	21.85	21.70
VectorScal-src	19.61	14.11	4.73	17.45	10.40	21.04	10.49	13.98
TempScal-src	15.12	8.37	4.12	10.86	8.23	13.25	8.07	9.72
CPCS	21.96	14.58	8.22	7.26	7.52	23.23	4.31	12.44
TransCal	6.58	11.28	14.28	10.21	12.67	7.18	13.10	10.76
Ensemble	19.74	16.66	9.08	16.51	12.48	19.31	14.03	15.40
PseudoCal (ours)	**3.40**	**4.44**	**1.50**	**2.23**	**0.81**	**2.12**	**1.79**	**2.33**
Oracle	0.86	1.75	1.21	1.11	0.78	0.57	1.06	1.05
Accuracy (%)	48.14	48.65	66.40	50.54	59.89	47.18	56.17	53.85

Table 24: ECE (%) of a closed-set UDA method MCD (Saito et al., 2018) on *DomainNet*.

Method	C → S	P → C	P → R	R → C	R → P	R → S	S → P	avg
No Calib.	12.97	9.47	3.80	9.65	7.01	12.89	7.80	9.08
MatrixScal-src	31.47	19.56	10.05	20.32	14.30	24.98	18.45	19.88
VectorScal-src	19.63	12.59	5.75	16.53	10.21	20.95	10.27	13.70
TempScal-src	11.61	5.39	4.06	7.58	7.19	10.79	6.74	7.62
CPCS	19.75	6.09	1.96	7.94	3.92	23.82	3.10	9.51
TransCal	19.44	21.53	27.45	21.44	25.19	18.45	24.79	22.61
Ensemble	11.60	7.54	2.86	6.95	5.35	11.07	5.19	7.22
PseudoCal (ours)	**1.66**	**3.60**	**1.01**	**0.93**	**1.11**	**1.73**	**1.21**	**1.61**
Oracle	0.62	1.81	0.56	0.85	0.91	0.73	1.03	0.93
Accuracy (%)	49.09	48.21	65.32	49.49	59.58	46.81	56.40	53.56

Table 25: ECE (%) of closed-set UDA methods on *Office-31*.

Method	ATDOC (Liang et al., 2021)					BNM (Cui et al., 2020)					MCC (Jin et al., 2020)				
	A → D	A → W	D → A	W → A	avg	A → D	A → W	D → A	W → A	avg	A → D	A → W	D → A	W → A	avg
No Calib.	4.59	6.66	11.43	12.91	8.90	11.12	8.27	24.60	22.22	16.55	6.18	7.80	18.60	19.97	13.14
MatrixScal-src	9.58	13.21	14.04	15.35	13.05	11.22	8.81	24.64	21.94	16.65	9.70	10.21	18.99	21.84	15.19
VectorScal-src	4.57	6.43	15.69	17.50	11.05	8.15	4.11	24.82	23.59	15.17	5.12	3.16	20.53	24.01	13.21
TempScal-src	**3.39**	4.18	24.37	20.41	13.09	9.23	4.98	26.15	21.55	15.48	3.79	3.00	22.07	20.70	12.39
CPCS	7.98	8.94	26.49	22.80	16.55	11.65	**2.02**	27.16	17.73	14.64	4.69	3.03	29.84	30.47	17.01
TransCal	14.21	14.64	13.27	11.02	13.29	**5.22**	2.70	16.00	13.72	9.41	3.77	3.91	5.57	7.49	5.19
Ensemble	3.60	**4.09**	9.04	10.53	6.82	6.92	4.63	19.99	19.56	12.78	3.07	4.88	17.18	17.78	10.73
PseudoCal (ours)	6.64	4.98	**3.22**	**4.47**	**4.83**	6.30	3.97	**10.75**	**8.21**	**7.31**	**2.68**	**2.82**	**4.50**	**4.71**	**3.68**
Oracle	2.49	3.15	1.90	2.35	2.47	2.65	1.40	2.63	2.41	2.27	2.36	2.67	2.42	2.05	2.38
Accuracy (%)	91.57	88.93	73.41	73.06	81.74	88.35	90.94	71.35	73.77	81.10	91.37	89.06	69.86	69.51	79.95

Table 26: ECE (%) of closed-set UDA methods on *Office-31*.

Method	CDAN (Long et al., 2018)					SAFN (Xu et al., 2019)					MCD (Saito et al., 2018)				
	A → D	A → W	D → A	W → A	avg	A → D	A → W	D → A	W → A	avg	A → D	A → W	D → A	W → A	avg
No Calib.	9.34	7.96	16.66	17.39	12.84	6.17	6.68	20.34	22.33	13.88	9.49	8.88	16.39	17.03	12.95
MatrixScal-src	11.90	14.91	17.21	21.12	16.29	9.49	13.97	20.56	23.43	16.86	9.83	13.49	17.86	20.28	15.37
VectorScal-src	6.04	3.60	17.67	25.37	13.17	3.22	**2.20**	21.07	23.59	12.52	5.87	4.61	17.75	20.52	12.19
TempScal-src	5.70	3.41	16.10	20.97	11.55	3.21	2.83	24.48	23.41	13.48	**3.44**	**2.36**	32.09	18.65	14.14
CPCS	30.95	5.67	**4.99**	29.95	17.89	8.21	18.21	24.18	22.12	18.18	11.85	19.01	32.45	22.92	21.56
TransCal	7.44	6.84	5.51	**4.18**	5.99	**3.04**	2.81	6.43	9.86	5.54	5.65	4.76	5.86	4.39	5.17
Ensemble	4.98	3.29	7.41	14.43	7.53	3.81	5.75	17.58	20.20	11.84	6.25	5.49	13.53	15.60	10.22
PseudoCal (ours)	**4.78**	**3.04**	6.39	6.78	**5.25**	7.92	5.51	**4.00**	**4.26**	**5.42**	5.97	5.33	**4.38**	**4.06**	**4.94**
Oracle	3.26	2.17	2.94	3.47	2.96	2.90	1.75	2.14	2.27	2.27	3.55	1.76	2.31	1.90	2.38
Accuracy (%)	87.15	87.17	64.82	67.23	76.59	89.96	88.55	69.33	68.58	79.11	86.14	85.53	67.52	66.63	76.46

Table 27: ECE (%) of a partial-set UDA method ATDOC (Liang et al., 2021) on *Office-Home*.

Method	Ar → Cl	Ar → Pr	Ar → Re	Cl → Ar	Cl → Pr	Cl → Re	Pr → Ar	Pr → Cl	Pr → Re	Re → Ar	Re → Cl	Re → Pr	avg
No Calib.	28.21	20.87	10.76	17.58	23.49	11.69	19.16	28.98	14.34	13.29	28.22	15.64	19.35
MatrixScal-src	35.85	19.37	13.42	29.69	30.20	21.94	21.96	37.00	14.83	19.36	34.96	16.94	24.63
VectorScal-src	25.87	15.83	7.46	18.37	20.96	11.63	19.96	33.03	12.36	11.16	26.57	11.61	17.90
TempScal-src	21.08	15.04	5.75	12.95	17.86	7.52	18.23	29.63	12.88	9.02	23.66	11.83	15.45
CPCS	28.34	27.40	19.28	14.37	6.27	10.86	32.51	39.04	13.75	11.28	21.84	7.92	19.41
TransCal	**4.36**	**5.07**	10.58	9.47	**4.98**	12.82	**9.12**	**5.81**	10.51	13.32	**5.34**	7.60	8.25
Ensemble	20.32	12.06	8.90	11.80	17.57	7.89	12.32	22.25	9.07	11.81	21.26	10.68	13.83
PseudoCal (ours)	9.15	7.08	**3.21**	**7.59**	7.53	**4.84**	11.80	12.79	**6.45**	**4.21**	10.75	**4.10**	**7.46**
Oracle	3.09	4.24	2.82	4.78	4.93	4.48	4.04	5.03	4.94	3.58	5.24	3.95	4.26
Accuracy (%)	51.46	64.99	77.19	61.89	61.34	73.44	59.50	49.01	70.51	67.68	51.64	71.43	63.34

Table 28: ECE (%) of a partial-set UDA method MCC (Jin et al., 2020) on *Office-Home*.

Method	Ar → Cl	Ar → Pr	Ar → Re	Cl → Ar	Cl → Pr	Cl → Re	Pr → Ar	Pr → Cl	Pr → Re	Re → Ar	Re → Cl	Re → Pr	avg
No Calib.	22.91	11.67	8.45	14.42	14.34	10.29	12.63	21.14	8.22	11.09	22.46	10.63	14.02
MatrixScal-src	35.16	19.13	14.89	29.94	30.26	25.30	24.67	34.81	14.78	18.58	34.09	15.73	24.78
VectorScal-src	19.52	9.73	6.05	12.79	14.23	11.07	16.13	26.53	9.03	9.29	20.18	7.95	13.54
TempScal-src	13.14	**5.37**	**3.05**	5.96	6.62	**4.21**	10.00	20.08	5.79	5.39	14.70	6.12	8.37
CPCS	19.34	10.62	4.00	4.25	**4.14**	12.00	28.24	37.75	16.08	5.70	27.24	12.51	15.16
TransCal	2.74	6.19	5.25	8.09	5.92	8.40	11.03	6.01	7.29	9.20	**4.06**	**4.13**	6.53
Ensemble	18.27	9.86	6.49	9.68	11.37	7.27	8.76	18.05	6.57	9.21	19.31	9.10	11.16
PseudoCal (ours)	**2.51**	7.86	4.70	**3.04**	6.70	5.78	**4.20**	**4.01**	**3.96**	**3.99**	4.36	6.23	**4.78**
Oracle	2.29	3.75	2.04	2.67	3.07	3.11	2.69	3.26	1.97	3.06	3.47	2.35	2.81
Accuracy (%)	51.10	74.17	81.56	62.53	66.72	73.16	63.27	50.03	79.96	70.80	53.91	79.33	67.21

Table 29: ECE (%) of a partial-set UDA method PADA (Cao et al., 2018) on *Office-Home*.

Method	Ar → Cl	Ar → Pr	Ar → Re	Cl → Ar	Cl → Pr	Cl → Re	Pr → Ar	Pr → Cl	Pr → Re	Re → Ar	Re → Cl	Re → Pr	avg
No Calib.	20.35	8.33	5.30	11.10	12.28	10.19	8.93	18.60	4.83	8.31	18.33	6.95	11.13
MatrixScal-src	36.55	24.04	16.23	34.97	33.22	28.87	27.26	37.58	16.54	20.45	35.41	16.45	27.30
VectorScal-src	20.53	7.22	4.71	12.28	13.91	13.44	22.41	31.95	9.35	9.07	19.86	8.57	14.44
TempScal-src	15.15	6.09	3.34	6.51	6.43	**4.64**	13.91	23.77	4.27	6.34	15.69	6.11	9.35
CPCS	24.22	30.26	24.81	9.80	7.37	43.23	28.84	39.45	14.97	34.57	4.55	14.27	23.03
TransCal	9.39	23.43	26.71	21.37	20.51	21.88	22.49	11.25	31.71	24.23	12.37	25.06	20.87
Ensemble	11.42	**4.97**	**2.88**	6.02	**4.54**	4.65	**3.76**	11.15	**4.24**	6.13	13.00	**3.79**	**6.38**
PseudoCal (ours)	**2.95**	12.31	7.51	**4.68**	10.14	5.38	5.77	**4.13**	7.19	**3.71**	**3.28**	9.85	6.41
Oracle	2.16	5.65	2.27	3.89	5.70	2.83	5.06	2.73	3.98	2.87	3.06	3.06	3.61
Accuracy (%)	43.82	59.83	72.45	51.70	52.32	58.14	51.52	40.66	69.02	63.73	47.70	71.54	56.87

Table 30: ECE (%) of a white-box source-free UDA method SHOT (Liang et al., 2020a) on *DomainNet*.

Method	C → S	P → C	P → R	R → C	R → P	R → S	S → P	avg
No Calib.	21.57	16.14	10.03	18.18	20.86	24.71	21.52	19.00
MatrixScal-src	27.18	19.67	12.49	19.13	16.99	21.60	20.35	19.63
VectorScal-src	17.79	13.95	6.46	19.31	16.25	22.17	13.20	15.59
TempScal-src	13.91	11.32	4.81	16.76	16.47	18.99	10.63	13.27
CPCS	12.52	7.28	4.93	13.64	10.86	16.57	9.10	10.70
TransCal	16.39	23.80	25.37	24.23	18.18	15.87	14.81	19.81
Ensemble	17.57	13.24	7.81	15.24	18.14	21.40	17.73	15.88
PseudoCal (ours)	**5.82**	**6.08**	**2.91**	**7.23**	**7.17**	**7.51**	**8.38**	**6.44**
Oracle	2.03	3.69	1.37	2.85	2.25	2.33	2.78	2.47
Accuracy (%)	59.80	66.79	78.34	66.25	66.08	59.48	62.88	65.66

Table 31: ECE (%) of a black-box source-free UDA method DINE (Liang et al., 2022) on *DomainNet*.

Method	C → S	P → C	P → R	R → C	R → P	R → S	S → P	avg
No Calib.	31.91	22.54	12.39	21.43	20.63	28.77	24.38	23.15
Ensemble	26.38	18.72	10.83	17.03	17.53	24.28	20.18	19.28
PseudoCal (ours)	**17.86**	**15.12**	**5.30**	**13.71**	**11.14**	**14.44**	**14.75**	**13.19**
Oracle	1.35	1.87	1.29	1.62	1.94	1.38	1.65	1.59
Accuracy (%)	54.26	63.00	80.69	64.52	67.13	56.75	63.81	64.31